The Henryk Niewodniczański
Institute of Nuclear Physics
Polish Academy of Sciences
ul. Radzikowskiego 152, 31-342 Kraków
http://www.ifj.edu.pl/badania/publikacje

Kraków, 2025

Application of MRI for myelin status differentiation in Multiple Sclerosis and in animal models of demyelination

Katarzyna Kalita

Monograph

Wydano nakładem Instytutu Fizyki Jądrowej im. Henryka Niewodniczańskiego
Polskiej Akademii Nauk
Kraków 2025
Recenzenci:
Prof. dr hab. Barbara Blicharska
Prof. dr hab. Kvetoslava Burda
ISBN: 978-83-63542-50-4 (print)
ISBN: 978-83-63542-51-1 (pdf)
DOI: https://doi.org/10.48733/978-83-63542-51-1

Abstract

Multiple Sclerosis (MS) is a chronic, incurable, autoimmune disease causing life-long physical and mental disability with focal areas of Central Nervous System (CNS) pathological changes appearing in conventional Magnetic Resonance Imaging techniques as "lesions". Lesions are heterogenous in terms of the dominant pathological processes, with possible involvement of remyelination to varying degree and at different stages. The interplay between demyelination an remyelination determines disease severity and upcoming physical and mental disability degree being also an indicative of therapy effectiveness. Lesion status identification is an important step of diagnosis and treatment efficacy determination. In MS except from a relatively well visible "lesions" also normal appearing white and grey matter are affected. Among conventional Magnetic Resonance Imaging (MRI) techniques, the degree of inability to differentiate between lesion myelination status is emphasized, while the experimental results of using more advanced imaging options such as Magnetization Transfer Ratio (MTR), Diffusion Weighted Imaging (DWI), Diffusion Kurtosis (DK) imaging and some lastly developed high b-value q-space imaging variants for the imaging of lesions is discussed. The goal of this paper is to emphasize currently developed, most promising magnetic resonance imaging modalities in lesion status differentiation in humans and in animal models, among which the cuprizone model seems to be most suitable for experimental myelin pathology research.

Characterization of the disease, epidemiology and diagnosis.

Multiple sclerosis (MS) is an autoimmune chronic inflammatory disease of the central nervous system (CNS). It affects currently more than 2,8 million people worldwide and is incurable (Walton et al., 2020). The major cause of the disease is unknown, however there are known risk factors including certain viral infections, age, sex (3/4 of patients are woman), geographical latitude (higher incidence in temperate climate), tobacco exposure and obesity. The disease has variable courses between individuals. Depending on the genetics and environmental factors or combination of both it can evolve in the direction of disease progression or relapse. Characteristic feature of the disease is the appearance of focal areas of inflammatory, demyelinating loci ('lesions') with heterogeneous axonal loss. It is not known which factors determine the direction of disease evolution (progression vs. relapse), however the existence of low inflammation level, few spinal cord lesions, many preserved axons and synapses, early treatment and younger age at disease onset are factors reducing the chances of disease progression. On the other site, chronic inflammation, many lesions (in the cortex and spinal cord), poor endogenous repair abilities, a high level of mitochondrial dysfunction and a high degree of axonal and synapse loss, together with delayed treatment and an older age at disease onset are the factors increasing the chance of disease progression (Reich et al., 2018).

The disease is characterized by periods of fully or partially reversible disability lasting usually days or weeks (Fig. 1). Typical syndromes at the disease onset include monocular visual loss due to optic neuritis, limb weakness or sensory loss caused by transverse myelitis, double vision due to brainstem malfunction, or ataxia caused by a cerebellar lesion (Brownlee et al., 2017). Usually, MS begins with a relapsing-remitting course (RRMS), in which relapses (new neurologic symptoms caused by inflammation and demyelination) are followed by periods of remission. After 10–20 years of the disease, especially when not treated, many of affected patients develop a "progressive" clinical course, characterized by impaired mobility and cognition. That condition is termed secondary progressive MS (SPMS). Some patients (15%) have a progressive course from the onset (primary progressive MS - PPMS). In this case relapses are not existent rather a progressive accumulation of clinical disability exists

(Boutitah-Benyaich et al., 2025, Cree et al., 2021, Goodin, 2025, Kilneova and Lublin, 2018, Lassmann et al., 2012,).

There are some available disease-modifying medications which can reduce the frequency of transient episodes of neurological disability and limit the accumulation of focal lesions, but no medication fully prevents or reverses progressive neurological deterioration leading to impaired neurological functions (i.e. ambulation, bladder control, impaired cognitive processing).

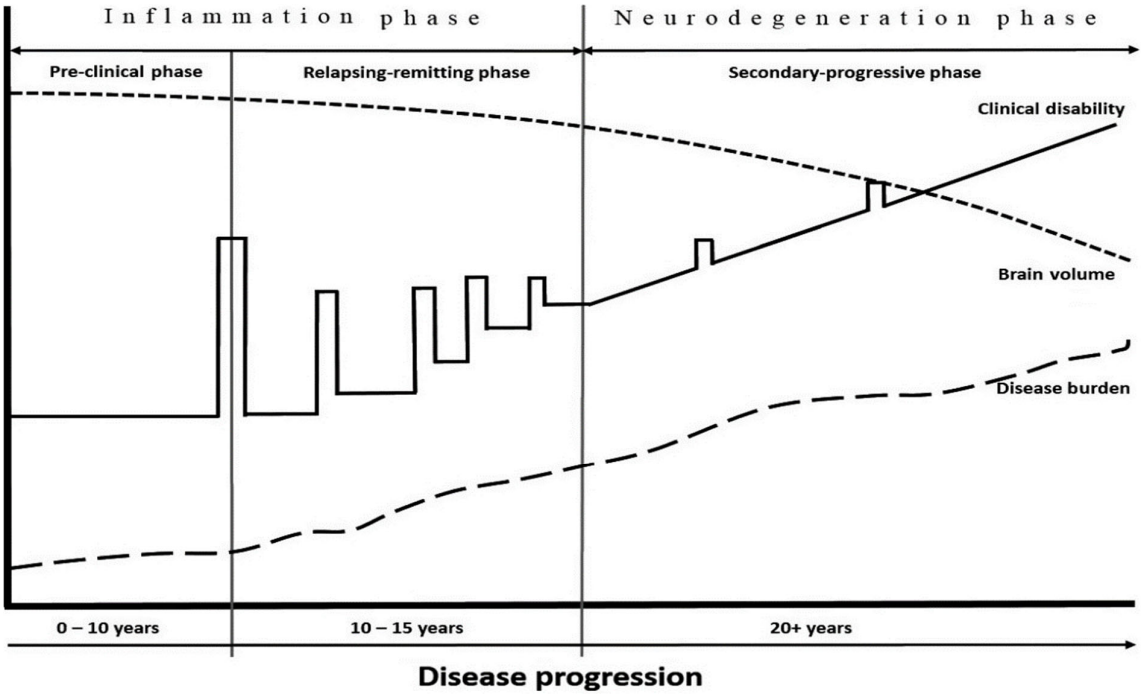

Fig. 1. The time course of Multiple Sclerosis development starting from silent pre-clinical phase with the absence of neurological symptoms usually lasting up to 10 years, through relapsing-remitting phase in which interleaved, variable periods of clinical relapses and remissions are present up to constantly increasing progression phase with concomitant worsening of clinical disability, disease burden increase and brain atrophy progression. Reprinted without changes with permission from Bou Fakhredin et al., 2016, https://doi.org/10.1111/1754-9485.12498, https://onlinelibrary.wiley.com/doi/10.1111/1754-9485.12498 License Number 6165001012170

The concept of “Multiple Sclerosis” was established more than 150 years ago. It reflects the nature of the disease which is dissemination of multiple lesions (“sclerotic plagues”) in space (white matter, gray matter, brainstem, spinal cord, optic nerve) and time. Multiplicity of sclerotic plagues in both dimensions: space and time is a fundamental step of the diagnosis. The current state of knowledge about this disease results primarily from the development of two research methods: immunohistochemistry (start in the early 50's and substantial improvement in the 90's), and magnetic resonance imaging in the early 80's when the implementation of MRI in the diagnosis of MS patients took place (Young et al., 1981).

Plaque-like sclerosis consists of focal areas of local inflammation, glial reaction and demyelination. In the disease onset, white matter demyelination in the forms of so called “early active WM lesions” is observed, mainly in MRI and biopsy results. Lesions are heterogenous by means of immune system components engagement and the amount of myelin component loss and also their remyelination status, since spontaneous re-myelination is immanent feature of the disease (Lucchinetti et al., 2000). Early active white matter lesions constitute three main lesion categories: with pattern I and II showing the presence of mononuclear phagocytes an T-cells infiltration. In pattern II also immunoglobulin and complement presence is observed. Pattern III with numerous apoptotic oligodendrocytes and inner myelin loops degeneration is detected in about 25% of biopsied lesions together with toxic and ischemic features, resembling viral infection (for a detailed diagram see Fig. 2 in the paper of Reich et al., 2018).

After an acute phase of inflammation, some intrinsic factors which are not well established can redirect affected brain and spinal cord loci into three main lesion categories: “remyelinated lesion” when axons in a lesion were able to reconstitute a thin myelin sheet in the repair process, “chronic inactive lesions” if inflammation was resolved without remyelination or “smoldering lesions“ in case of continuously present inflammation and slow myelin degeneration. First two types are predominantly present in RRMS, while the last category is most common in progressive MS. What factor determines long term fate of a lesion is not well understood. It is also not established whether lesions can remyelinate in case of

smoldering ones and if remyelinated lesions have higher susceptibility to recurrent demyelination (Reich et al., 2018).

The primary target of autoimmune destruction are oligodendrocytes (OLs) – axonal wrapping cells responsible for maintaining saltatory conduction in the CNS. Apart from their effect on conduction, oligodendrocytes forming the myelin sheath also provides nutrition, particularly lactate, to the underlying axons supporting high energy demands of the axonal transport (Fünfschilling et al., 2012, Saab and Nave, 2017). Another process crucial for axonal function and integrity is potassium clearance, through oligodendrocyte-specific potassium ion channels (Schrimer et al., 2018). In MS, under the influence of an unknown trigger, immune cells of the host attack myelin sheath's own antigens, developing inflammation that results in concomitant axonal demyelination and degeneration. Myelin is present also in gray matter (GM) so demyelination and lesions are also present in GM. In the cortex, about a half of cortical lesions are perivascular, and inflamed vessel is close to leukocortical junction, so inflammation involves both gray and white matter. Cortical lesions are less inflammatory and have lower Brain Blood Barrier (BBB) permeability (Peterson et al., 2001). Local and peripheral inflammation is a main feature of MS: the presence of activated lymphocytes, macrophages and microglia is described in brain and spinal cord lesions (Maggi et al., 2014).

Blood brain barrier breakdown is also a very dominant feature of early MS lesion – evidence suggest that BBB disruption precedes inflammatory demyelination in animal models (Maggi et al., 2014) and possibly in human. Autoimmune inflammation leads to further pathological event cascade: axonal damage (including transection), neuronal apoptosis and atrophy, gray matter degeneration and vascular inflammation leading to many metabolic and functional abnormalities (Trapp et al., 1998, Peterson et al., 2001, Aktas., 2005, Klineova and Lubin, 2018). Demyelination is also present in the spinal cord and the optic nerve (Reich et al., 2018).

Beyond focal changes visible in pathologically altered CNS structure, white and grey matter areas distant to the focal lesion side show subtle but important signs of tissue damage: microglia activation, abnormal blood vessels, increased expression of genes

related to proteolytic processing, or a decreased expression of genes regulating oligodendrocyte survival (Huynh et al., 2014). Since these white and grey matter regions are not healthy, even though they appear as such on conventional MRI, they are described as normal-appearing white matter (NAWM) and normal appearing grey matter (NAGM).

In RRMS course, neurological function can fully recover after a relapse but some degenerative processes are triggered by focal lesions that are not yet apparent during the early disease phase. These slow-burning degenerative processes are believed to be driven by local, innate immune cells. In SPMS two important pathogenetic factors change: the activity of the adaptive immune system decreases, resulting in a lower frequency of clinically detectable relapses (Tremlett et al., 2008) and as a result of damage accumulation, the slow-burning degenerative process, after reaching a certain threshold, is manifesting clinically as significant disability (Fig. 1). Delayed clinical manifestation of this slow-burning neurodegeneration is possibly caused by neuronal plasticity processes allowing for the transfer of damaged or degenerated neurons function to neighboring, non-affected neurons (Schoonheim et al., 2010, Enzinger et al., 2016). On the other hand, the destruction of a single neuron or a group of neurons does not necessarily result in overt clinical deficits in RRMS, but at the transition phase from RRMS to SPMS, when many neurons are already lost, the subsequent damage to additional neuronal structures results in visible accumulating clinical deficits. Adaptive immunity has a dominant role in RRMS, while during the progressive phase of the disease brain resident innate immune cells are the major and direct tissue damage source. Axonal damage and concomitant failure of remyelination aggravates disease course.

To summarize, MS is a chronic, incurable, autoimmune disease that causes life-long physical and mental disability with focal areas of CNS inflammation, demyelination and tissue damage. Lesion distribution and dissemination in space and time is a cornerstone of disease diagnosis. Lesions are heterogenous in terms of dominant pathological processes occurring including inflammation, BBB breakdown, demyelination, axonal injury or remyelination domination. Lesion status identification is important in the research of underlying pathological mechanisms of

MS but also for the diagnosis and treatment efficacy determination. In MS except from a relatively well visible "lesions" also normal appearing white and grey matter are affected. The most sensitive method of lesion detection is Magnetic Resonance Imaging. The goal of this paper is to emphasize currently developed, most promising magnetic resonance imaging modalities in lesion status detection and differentiation in animal models best suitable for experimental MS research.

Animal models of multiple sclerosis

Animal models of MS have greatly enhanced knowledge of the pathophysiology of MS disease. The most extensively used are Experimental Autoimmune Encephalomyelitis (EAE model), toxic models (cuprizone, lysolecitine, ethidium bromide) and viral (infectious models). Each of these animal models provides different potential routes to investigate MS disease processes.

Most widely used animal model is experimental autoimmune encephalomyelitis (EAE). In this model, T cells are either induced by presenting the animal's own myelin antigen, or transfused into the animal. It's a model of chronic inflammation which can be induced in many variants: depending on animal species and strain and also immunogen used, it displays monophasic, relapsing–remitting, chronic-progressive or chronic-relapsing disease courses (Buttigieg et al., 2023). The diverse types of EAE models all together present the spectrum of clinical phenotypes of MS (Kipp et al., 2012). In clinical MS and in animal EAE, the presence of T-cells (CD4 + and CD8 +) is observed (Steinman and Zamvil, 2005). Leukocyte migration to the CNS is also similar in EAE to that in MS patients, with activated leukocytes adhering to endothelial cells and migrating through the glial barrier into the CNS parenchyma. (Agrawal et al., 2011). In the MRI results, in both animal EAE and human MS, lesion load does not directly correspond to the level of clinical disability (Wuerfel et al., 2007, Ladopoulos et al., 2025).

Despite EAE model reflect a huge range of important MS features, such as inflammation and axonal loss, its usefulness for understanding demyelination and remyelination is low, because it has several disadvantages: demyelination and

neurodegeneration are not consistent across the studies, the size and location of lesions are difficult to predict, the detection of demyelination and remyelination may be compromised by their simultaneous appearance (Constantinescu et al., 2011, Lubetzky et al., 2020, Buttigieg et al., 2023).

Viral models are very complex and not well adapted to the study of demyelination and remyelination (DePaula-Silva et al., 2017, Lassmann and Bradl, 2017).

Toxic models do not contain the inflammatory component of multiple sclerosis but are extremely useful for discovering the mechanisms of demyelination and remyelination. Ethidium bromide (EtBr) induces oligodendrocyte and astrocyte death, with focal demyelination at the site of injection, followed by extensive remyelination. Lysophosphatidylcholine (LPC) damages the myelin sheaths at the site of injection, which is followed by efficient remyelination (Lassman and Bradl, 2017). Lysophosphatidylcholine and ethidium bromide both give rise to focal areas of demyelination, while cuprizone model delivers more disseminated myelin alterations (Plemel et al., 2017, Lubetzki et al., 2020).

Cuprizone (CPZ) model provides insight into demyelination and remyelination processes. For both modalities induction, cuprizone (bis-cyclohexanone oxaldihydrazone), a copper chelator, is administered to a mouse chow at 0.2–0.3% concentration, for a defined number of weeks. That treatment has a potential to induce either transient or chronic demyelination depending on feeding time. Demyelination is observed in relatively predictable brain areas such corpus callosum, hippocampus, cerebral and cerebellar cortex, superior cerebral peduncles (Skripuletz et al., 2010, Gudi et al., 2009). The time course of cuprizone- induced demyelination and remyelination in a medial corpus callosum of a C57BL/6 mice fed with cuprizone is schematically represented in Fig. 2.

Cuprizone intake selectively alters the homeostasis of oligodendrocytes, leading to their apoptotic death and subsequent loss of myelin sheath (Skripuletz et al., 2010). The susceptibility of OLs might be caused by mitochondrial imbalance (Acs et al., 2013, Zirngibl et al., 2022). CPZ diet leads to activation of microglia and strong astrogliosis preceding the demyelination (Gudi et al., 2009). Demyelination in this

model had been also evoked in rats (Adamo et al., 2006, Li et al., 2013, Serra-de-Oliveira et al., 2015). Cuprizone intoxication follows a certain pattern of myelin loss and, consequently, oligodendrocyte loss: during the first 3-4 weeks, it is accompanied by the recruitment of microglia, macrophages and astrocytes (acute phase), and oligodendrocytes progenitor cells accumulate at the sites of lesions, and after 5-6 weeks, demyelination is subacute and spontaneous remyelination begins (Falangola et al., 2014).

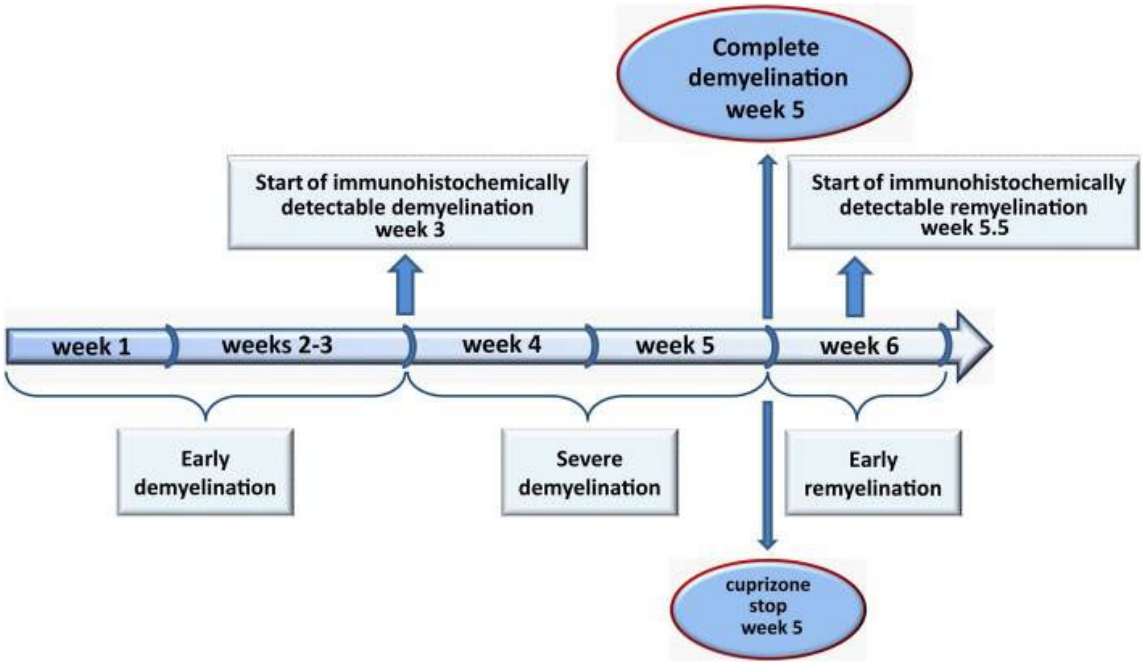

Fig. 2. Schematic representation of the course of demyelination and remyelination in the medial corpus callosum of C57BL/6 mice fed with cuprizone for 5 weeks. Reprinted without changes from Gudi et al., 2014, doi: 10.3389/fncel.2014.00073. https://www.frontiersin.org/journals/cellularneuroscience/articles/10.3389/fncel.2014.00073/full, https://creativecommons.org/licenses/by/4.0/

The remyelination begins within a week after toxin arrest and is accomplished by oligodendrocyte precursor cells recruitment, migration and maturation (Baxi et al., 2017, Praet et al., 2014). If cuprizone administration is prolonged up to more than twelve weeks chronic-demyelination can be evoked (Ludwin., 1980). For more detailed visualization and description of cuprizone – induced pathological cellular processes see Fig. 3.

Very precious feature of cuprizone model is a distinct temporal pattern of demyelination in white and grey matter (Wegerland et al., 2012). Another important feature is the presence of regional differences within the main white matter tract (i.e. the corpus callosum), allowing simultaneous study of several degrees of demyelination in the same individual (Praet et al., 2014).

Cuprizone is very effective in induction demyelination, however its mechanism of action remains unknown – it's the main weakness of this model. After cuprizone was administered, mitochondrial degradation and ferroptosis (Jhelum et al., 2020) were observed, as well as an endoplasmic reticulum stress response (Fishbach et al., 2019). These have been suggested as potential direct causes of oligodendrocyte degradation.

This model is not suitable to study autoimmune mediated demyelination, however it is very useful for investigation cellular and molecular mechanisms during de- and remyelination independently of interactions with peripheral immune cells (Gudi et al., 2014).

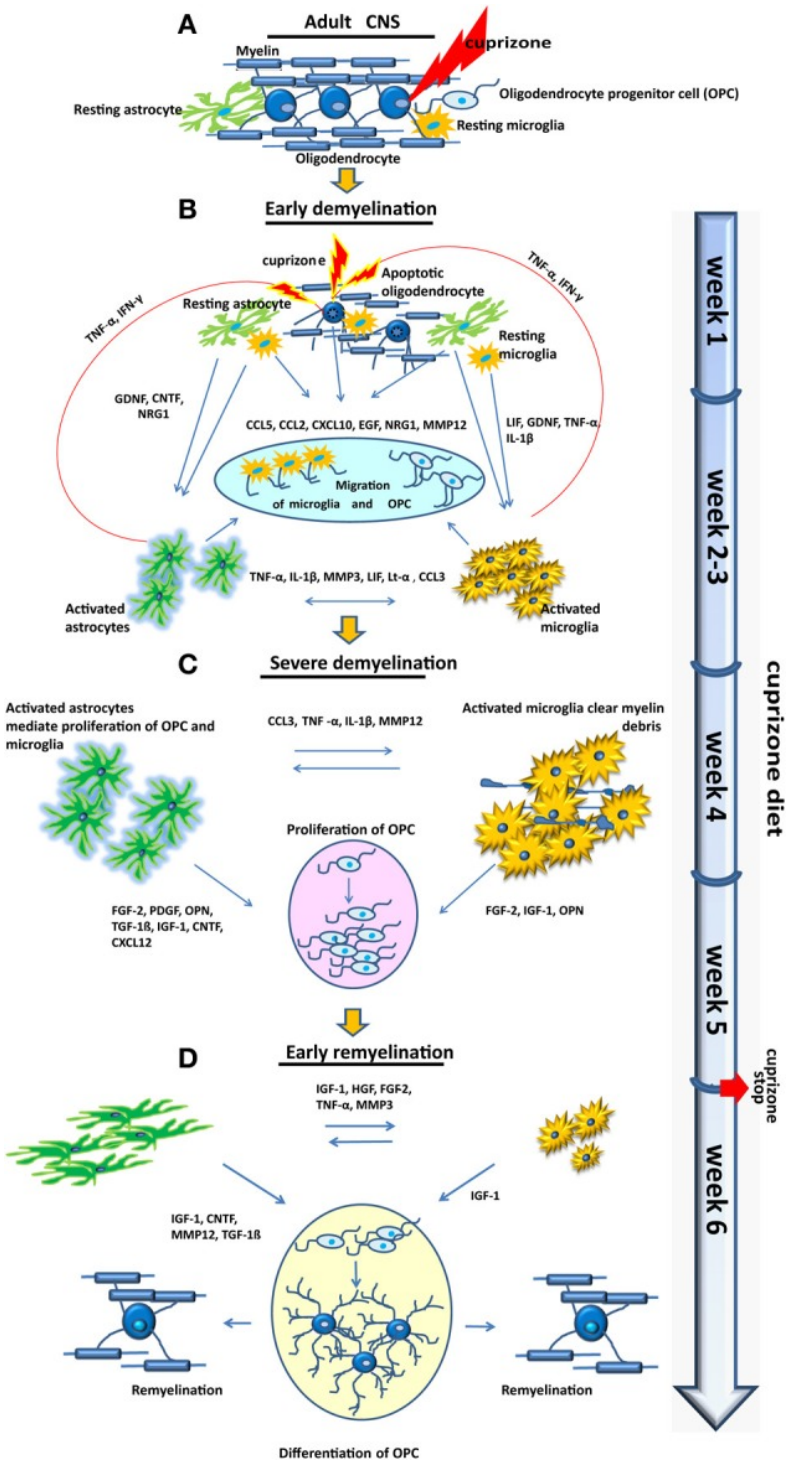

Fig. 3. The diagram of cellular and molecular response to cuprizone administration in the medial corpus callosum leading to de- and remyelination. (A) Healthy CNS tissue glial cells distribution: blue round-shaped cells are oligodendrocytes forming myelin sheath on adjacent neurons. (B) During 1–3 weeks of cuprizone intoxication,

early demyelination occurs on the way of mature oligodendrocytes apoptosis already present during the first week of cuprizone feeding. Microglia are activated, initiating inflammatory and reparative processes together with astrocytes. Numerous cellular transduction factors initiating attraction and activation of microglia, astrocytes and oligodendrocyte precursor cells (OPC) are released in the first week of intoxication. In the next 2 weeks early demyelination occurs with maintenance of the inflammatory activity. After three weeks oligodendrocytes are almost completely destroyed (C) Weeks 3.5–5 are a period of severe demyelination. Activated microglia begin to clear myelin debris. Several cellular signal transduction factors produced by activated astrocytes and microglia are supporting phagocytosis and promoting proliferation of OPC. At week 5 almost all axons in the medial corpus callosum are demyelinated. (D) In weeks 5-6 after cuprizone cessation early remyelination begins. In this stage the amount of activated microglia begins to decline. Astrocytes are still activated but change their morphology. OPC differentiate and begin to remyelinate nude axons. Reprinted without changes with permission from Gudi et al., 2014, doi: 10.3389/fncel.2014.00073.

https://www.frontiersin.org/journals/cellular-neuroscience/articles/10.3389/fncel.2014.00073/full, https://creativecommons.org/licenses/by/4.0/

In the modification of original cuprizone – induced demyelination model simultaneous administration of rapamycin, antibiotic known to reduce remyelination after intraperitoneal injection, was proposed. When administered together, cuprizone and rapamycin produce more complete and consistent demyelination with simultaneous slowed rate of remyelination (Sachs et al., 2014). In another modification, gavage administration of a particular dose of cuprizone induces substantial dramatic demyelination which is followed by remyelination after 9 days of feeding cessation. The authors claim that this approach results in increased effectiveness of remyelination and more reproducible results (Zhen et al., 2017).

To conclude, among multiplicity of animal models of MS to study demyelination and remyelination processes using different MRI techniques, the best suited are toxic models, among which cuprizone model seems to be the best option. The simplicity to achieve reliable, consistent demyelination and opportunity to study different myelination events across brain structures makes cuprizone animal model exceptional for MRI. In this model demyelination can be easily evoked and managed in terms of controlling its course and severity (acute, prolonged, chronic, early, late phase, extensive remyelination, spontaneous remyelination). Therefore, this model is excellent to study MRI appearance of de- and re-myelination in terms of sensitivity, specificity and reproducibility. The main weakness of this model is cuprizone's unknown mechanism of action while the main advantage of this model is its simplicity and multiplicity of focal de- and remyelination loci, making it a perfect tool for studying MRI appearance of demyelination using different imaging modalities.

At the disease onset active lesions (plaques) are characterized by focal inflammation (T-lymphocytes, monocytes, and macrophages), BBB breakdown and demyelination (Love and Louis, 2008). At this stage, axons are usually spared, however extensive axonal injury is observed (Wu and Alvarez, 2011). As the disease progresses, lesional cell number decreases, glial scarring and a loss of myelin becomes prominent: lesions are starting to become heterogenous. Based on myelin protein loss, the location and extension of plaques, the patterns of oligodendrocyte destruction, and the presence of complement activation, four different patterns of demyelination can be distinguished (Keegan et al., 2005, Lucchinetti et al., 2000). Spontaneous remyelination is an immanent feature of MS and also a goal for MS therapies. For the evaluation of disease evolution and treatment efficacy, finding noninvasive diagnostic tool which distinguishes between the amount of an ongoing de- and remyelination process is very important. Therefore, the focus of interest is to find non-invasive method for determining not only the content of myelin, but also its quality in terms of proper spatial organization around the axon.

Conventional MRI techniques: information about the number, size and location of lesions in the brain.

The first report of MRI use in MS patients took place in 1981. In total of 10 examined patients, Computer Tomography (CT) detected 19 brain lesions, while MRI detected 112 additional lesions, not visible in earlier CT brain scans (Young et al., 1981). Formally MRI was introduced to worldwide accepted McDonald diagnostic criteria of MS in 2001 as the best imaging modality identifying "demyelinated" MS lesions (McDonald et al., 2001).

MRI criteria for MS are based on the presence of focal lesions in the white matter (WM) of the CNS, which are considered typical for this condition in terms of distribution, morphology, evolution, and signal abnormalities on conventional MRI sequences (e.g., T2-weighted, pre- and post-contrast T1-weighted scans). These criteria are revised in the paper of Filippi et al., (2016).

Early inflammatory lesions appear bright on T1-weighted gadolinium (Gd) enhanced (T1W-Gd) images under two conditions: the degree of inflammation is big enough to disrupt BBB barrier and cause concomitant disturbances in glymphatic system and also gadolinium injection is temporally adjusted to MRI acquisition time to “catch” gadolinium ability to diffuse through damaged BBB and glymphatic system (Bou et al., 2018). T1W-Gd imaging is the gold standard to determine the number and size of early inflammatory lesions. Within following weeks of disease progression (median 2 weeks, Cotton et al. 2003) up to 6 weeks the enhancement disappears but such lesions are visible on T2W images as hyperintense areas (Filippi et al., 2019). Such lesions are radiologically defined as ‘chronic’ and remain visible on both T2-weighted (T2W) and T1-weighted (T1W) images, and the extent of T1 hypointensity may correlate with axonal degeneration in the white matter (van Waesberghe et al., 1999). Histologically, they have a heterogenous level of remyelination, ranging from low to completely remyelinated and low inflammatory activity. The illustrative time course of Gd-enhanced lesions number in MS course together with other pathological features such as T2 lesions number, brain atrophy progression, GM and NAWM injury progression is presented in Fig. 4.

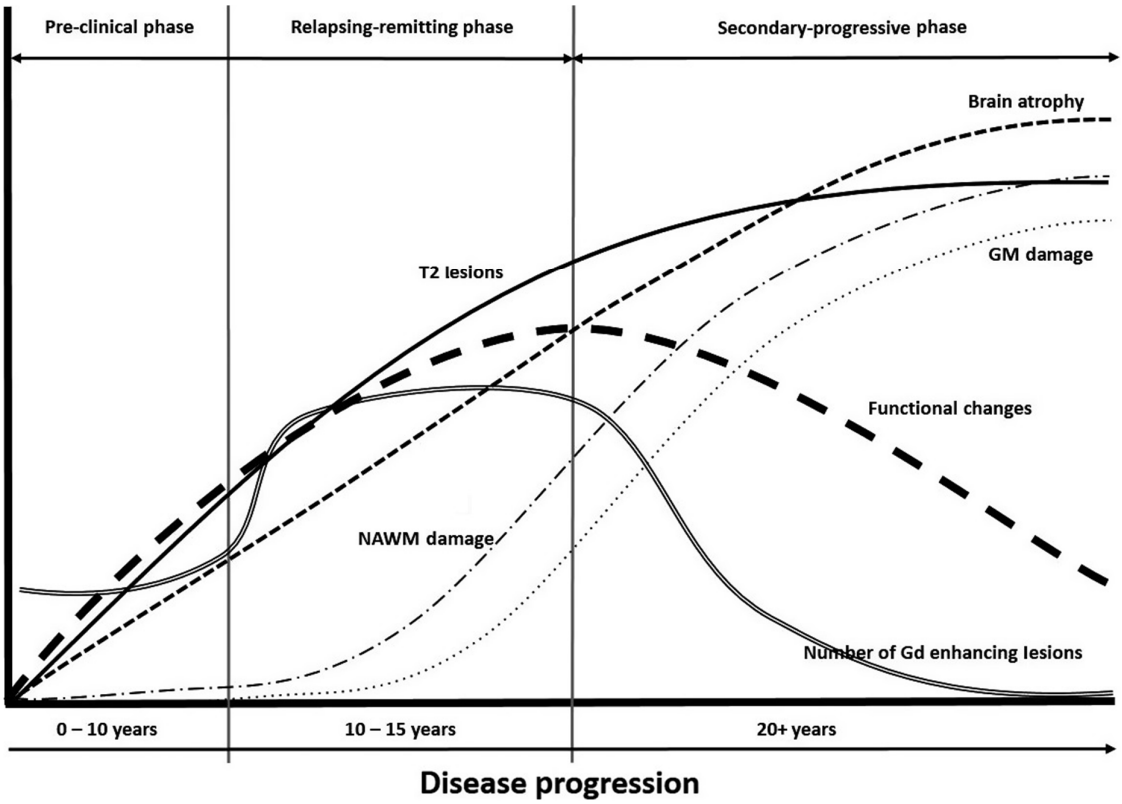

Fig. 4. Brain atrophy, T2 lesions, NAWM damage, WM damage, functional changes and the number of Gd-enhancing lesions relative to disease progression and which phase of the MS cycle they are classified under. Reprinted without changes with permission from Bou Fakhredin et al., 2016, doi: 10.1111/1754-9485.12498. https://onlinelibrary.wiley.com/doi/10.1111/1754-9485.12498, License Number 6165001012170.

In the evolution of this disease, some (approximately one third) of the previously T1W-bright lesions turn into so-called 'black holes' over time. These are dark spots on the T1W image, also known as 'chronic black holes'. Some lesions evolve in partially/completely remyelinated lesions. Complete remyelinated lesions disappears on both T1W or T2W images, and this disappearance is attributed to complete remyelination with no residual inflammation or edema. Some of completely remyelinated lesions appear still as hyperintense on T2W images - in this case standard T2W imaging does not reflect actual clinical status of the lesion,

probably because not complete spatial restoration of water compartments in the damaged tissue (Zivadinov et al., 2008).

Conventional MRI imaging detects demyelinated lesions as hyperintense areas on T2W images and hypointense areas on T1W images. This MRI appearance is also typical of partially remyelinated lesions. Fully remyelinated lesions in majority of cases appears the same on T2W images and have only slightly weaker signal on T1W images where they appear as shadow plaques (Zivadinov et al., 2008). In general, demyelinated and partially remyelinated lesions appear similar on T1W and T2W weighted images. T1W imaging more clearly distinguishes between fully remyelinated and demyelinated lesions (spots are hypointense or isointense in remyelinated lesions and strongly hypointense in demyelinated lesions). In some cases, completely remyelinated areas appear hyperintense, whereas in other individuals, they can disappear completely (Barkhof et al., 2003; Patrikios, 2006). In this case, the MRI result does not reflect the patient's clinical status (Zivadinov et al., 2008).

As the process of remyelination is extensive in around 20% of patients and can cover up to 96% of the total lesion area (Patrikos et al., 2006) it is very important to address the issue of qualitative detection of active spots in the brain with simultaneous evaluation of their myelination status. In patients with MS, the cortex has a much higher remyelination capability than the white matter. Remyelination has been detected even in elderly patients, so it should be considered a primary outcome measure in clinical trials testing new therapies. (Chang et al., 2012).

The phenomenon of demyelination and following remyelination is also a typical feature in animal models of MS. In remyelinated lesions axonal density is higher and axonal markers of neurodegeneration are decreased suggesting its neuroprotecting effect (Schulz et al., 2017, Kornek et al., 2000). Remyelination promotes axonal survival, as revealed by a study of cuprizone-induced demyelination in mice (Irvine & Blakemore, 2008). It also helps preserve axonal density and integrity in the EAE mouse model (Mei et al., 2016), and is a cause of recovery from neurological deficits in a cat model of remyelination (Duncan et al., 2009). In progressive multiple

sclerosis where remyelination in GM is extensive, remyelination has been proved to promote functional network restoration (Battefeld et al., 2016).

In comparison to T2W imaging, fluid-attenuated inversion recovery (FLAIR) sequence can increase lesion detectability especially in periventricular, juxtacortical, and infratentorial areas which are typical MS lesions locations. Thanks to the nulling the CSF signal (with the use of an inversion pulse, preceding image data collection by appropriately adjusted inversion time - TI), improved visualization of the brain is possible with better distinction of brain healthy tissue from lesions (De Coene et al., 1992). This results in strong T2W enhancement and optimised contrast between GM and WM, improving lesion visibility (Kates et al., 1996).

T1-weighted FLAIR imaging also has several advantages over conventional T1W Fast Spin Echo (FSE) pulse sequences. It provides improved contrast between lesions and the surrounding tissue, as well as between WM and GM, offering improved detectability of MS lesions. However, a higher noise level is observed when comparing the T1W FLAIR sequence to the T1W TSE (Bergamino et al., 2019).

Remyelination is a marker of ongoing healing processes leading to tissue performance improvement. Remyelination detection might be a marker of positive response to the applied therapy. Thus, imaging remyelination is of great importance to assess the disease course, and response to treatment. This phenomenon cannot be reliably assessed in patients using conventional MRI sequences but there is a convincing body of evidence, that some more advanced imaging options allow for more direct and thus more sensitive measure of tissue myelination status. Those techniques seem to be more sensitive to myelin presence and/or even specific myelin spatial organization. These include advanced diffusion-based imaging options and Magnetization Transfer Imaging.

MPRAGE sequence for Myelin Contrast Ratio (MCR) maps.

An MP-RAGE (Magnetization Prepared - RApid Gradient Echo) sequence can be applied for the whole rat's brain scanning to detect demyelination after cuprizone administration (Oakden et al, 2017). MPRAGE sequence was used together with T1W

image acquisition and corresponding Proton Density Weighted (PDW) imaging. Flash image to correct for B1 field (radio frequency field) receive homogeneity in T1W images allowing for Myelin Contrast Ratio (MCR) maps calculation of full mouse brain. The total acquisition time was approximately 2 hours. MCR maps were collected at 2, 4, 6 and 8 weeks following cuprizone diet and revealed a significant demyelination confirmed by histological results starting from 4-th week. At that time point, a 25% signal loss visible in cerebellar nuclei and other brain structures including WM an GM was observed in MCR maps (Oakden et al., 2017). This imaging option seems to be fast and sensitive to myelin content in the rodent brain (Oakden et al., 2017).

Direct myelin water detection – Myelin Water Fraction (MWF) imaging.

Myelin Water Imaging is a quantitative technique based on a concept that total MRI signal comes from water protons. Since individual protons may experience different microscopic environments, depending on their physical location in tissue, they have different T2 relaxation times. Because the entire MRI signal comes from different non-exchanging tissue compartments, the T2 relaxation decay curve of that signal is the sum of exponential decays with amplitudes proportional to the relative amounts of water in particular compartments. The physical size of a particular water reservoir determines T2 relaxation time within this reservoir, because water in tight compartments has shorter T2 relaxation time in comparison to water protons in in less tightly confined spaces. As shown in Fig. 5, the tissue heterogenous T2 decay signal can be separated into signals from: (i) water trapped between myelin bilayers (myelin water), (ii) intra/extracellular water and (iii) additional longer T2 components that are seen in some neurological diseases including MS (T2 ~200–800 ms), and CSF (T2 of ~2000 ms), (MacKay et al., 1994, Laule et al., 2007).

In human MS brains MWF correlated well qualitatively and quantitatively with histological myelin staining at 7T postmortem study (Laule et a., 2007). Myelin water has been shown to decrease in MS lesions to a variable degree (Laule et al., 2004, MacKay et al., 1994, Vavasour et al., 1998), and be reduced in NAWM of MS patients when compared to healthy controls (Laule et al., 2004). A relatively recent study also

revealed the possibility of age-related changes to the MWF (Billiet et al., 2015). Study performed in MS patients confirmed that lesions have decreased MWF values which was increasing in the disease course, suggesting remyelination (Vargas et al., 2015). However, the MWF use in a clinical diagnostic of myelination status is questionable because this modality is not specific to healthy myelin, as it cannot distinguish myelin debris from intact myelin sheaths (MacKay and Laule, 2016) and shows a better correlation with myelin status in a higher (7T) magnetic field (Laule et al., 2008) rarely available in clinical research. On the other hand, high resolution preclinical scanners equipped with strong magnetic field gradients that may cause spurious signal decay due to molecular diffusion which leads to T2 values underestimation. An important limitation in MWF imaging in clinical practice is the acquisition time (whole brain scan with 5 mm slice takes around 30 min, Ortiz et al., 2015) and post - processing. However, a recent study has found a good agreement between data-driven MWF values (in 7T magnetic field) and histology evaluation in cuprizone mice when particular data – driven multicomponent analysis was applied (Omer et al., 2025).

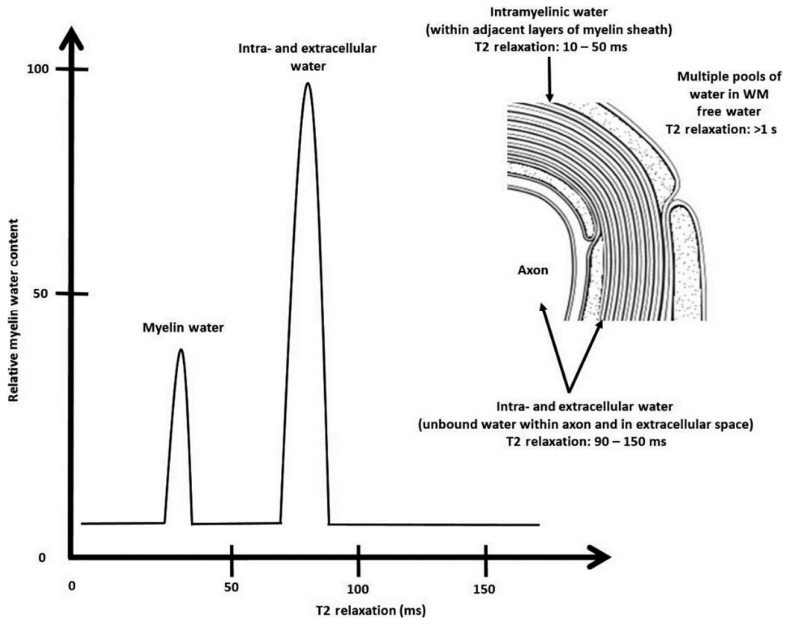

Fig.5. A schematic visualization of the main assumption of the multicomponent T2 measure to extract information regarding the quantitative myelin water amount (MWF), based on the fact that in individual tissue compartments T2 of water

hydrogens is differentiated and in the process of signal can be quantified. Reprinted without changes-with permission from Bou Fakhredin et al., 2016, doi: 10.1111/1754-9485.12498, https://onlinelibrary.wiley.com/doi/10.1111/1754-9485.12498 License Number 6165001012170.

In post mortem evaluation of different types of lesions (chronic demyelinated vs remyelinated lesions) in MS brains, MWF correlated better with remyelination than MTR (Wiggermann et al., 2023).

Advanced MRI techniques – Magnetization Transfer Imaging (MTI).

Magnetization Transfer Imaging (MTI) or Magnetization Transfer Ratio (MTR) imaging is a technique based on the very short T2 relaxation time (off resonance frequency) of protons bound to big macromolecules, such as myelin. It is so called "restricted proton pool" with short T2 impossible to be imaged directly using MRI, with T_{2r}<100μs. Using special pulse sequences that allow for the applying of an off-resonance frequency, it is possible to saturate preferentially immobile protons of macromolecules (Wolf and Balaban, 1989, Balaban and Ceckler, 1992). This magnetization energy is then transferred to mobile protons (free proton pool) with long T_2 (T_{2f}>10ms) and reduces their signal intensity. The relative difference in signal intensity with and without magnetization transfer, i.e. the magnetization transfer ratio is then calculated. Tissues with a large number of macromolecules – bound protons will show a large signal intensity decrease following the application of saturation pulse. Tissues with few restricted protons will have a very small MT effect. Thus, a demyelination process should be reflected on MTR images, thus that method was proposed to be useful for differentiating between lesion types in MS. An advanced extension of MTR imaging is quantitative magnetization transfer (qMT) imaging (Sled and Pike, 2001). This method allows for calculation of the macromolecular protons ratio (F) describing relative size of the restricted proton pool. That value represents protons from all the nonaqueous tissue thus representing myelin. This way a link between changes in (F) and changes in myelin can be made within WM. Also other quantitative parameters such as magnetization exchange rate

(kf), and relaxation parameters of the free and restricted pools (R1f, T2f, and T2r) can be extracted (Sled and Pike, 2001).

WM lesions of MS patients are characterized by reduced MTR signal (Tomiak et al., 1992). The MTR signal is also reduced in NAMW but these changes are subtle comparing to much more pronounced lesional MTR signal change (Dousset et al., 1992, Filippi et al., 1995). As Dousset et al. (1992) first suggested that the wide range of the MTR signal may indicate different myelination status of MS lesions. In the majority of studies the differences in the MTR in lesions of different ages or classes were detected (Tomiak et al., 1994, Campi et al., 1996, Hiehle et al., 1994). MTR correlates with both demyelination and remyelination in MS lesions (Filippi et al., 2012; Absinta et al., 2016; Laule and Moore, 2018). It has also been demonstrated that partial remyelination can occur and can be localized either to specific parts of the lesion (most commonly the lesion edge) or to the whole lesion (Filippi et al., 2019).

MTR imaging is very sensitive to pathological tissue changes as revealed by the research of NAWM of MS patients. NAWM are white matter regions in which there are no visible WM lesions. In reality in MS patients a big area of that tissue contains different abnormalities which are more prominent in the proximity of lesion and are becoming more discreate with increased distance from visible lesion (Vrenken et al., 2006). NAWM changes are more prominent in relapse – onset and in patients with clinically isolated syndrome (Soromani and Pradini, 2017). Post mortem microscopic evaluation of NAWM shows presence of diffuse microglia activation, gliosis, axonal loss, decreased axonal density. The majority of axonal deterioration manifests in the corpus callosum compared to other areas of the brain. (Evangelou et al., 2000, Ludwin., 2006). In MRI, abnormalities in NAWM can be identified before the appearance of inflammatory lesions. Among other MRI metrics, reduced MTR is present (Filippi et al., 1998).

In quite recent study, MTR in NAWM of MS patients was proved to be sensitive enough to detect very early, nonvisible pathological changes preceding lesion formation and being indicative for future lesion formation (Elliot et al., 2021). In this study retrospective analysis of NAWM in a huge cohort of MS patients revealed that

tissue state abnormalities may be detected as early as 6 months prior to a lesion formation: decreased nMTR (normalized Magnetization Transfer Ratio) simultaneously with higher nT_2 (normalized T_2 map) intensity was observed in pre-lesion NAWM up to 24 weeks prior to the appearance of new lesions. Both differences were detected in comparison to overall and spatially matched contralateral NAWM. No significant alterations were detected in nT_1 (normalized T_1 maps) or fractional anisotropy. These NAWM abnormalities are more pronounced at locations with high likelihood of developing subsequent MS lesions, like periventricular areas (Elliott et al., 2021). Because the formation of new lesions is a pathological marker of disease activity in multiple sclerosis, this study is very important as it proved the ability of the MRI modality (MTI) to predict upcoming disease relapse.

Studies using MTI have shown a concomitant reduction in MTR with ongoing demyelination in rodents and monkeys (Deloire-Grassin et al., 2000; Dousset et al., 1995; McCreary et al., 2009). However, the differences in MTR changes with remyelination are observed across different studies. One study is reporting MTR increase with remyelination in lysolecithin-injected rats (Deloire-Grassin et al., 2000), while the other did not observe a change in MTR over the disease course in the same model (McCreary et al., 2009). In both studies MTR signal values do not return to the baseline level, reflecting incomplete remyelination confirmed by histology (Deloire-Grassin et al., 2000; McCreary et al., 2009).

Another study used in vivo T2W and MT imaging acquired weekly in cuprizone – treated mice resulting in significant increase in signal intensity in T2W images and reduced MTR in the corpus callosum, starting at 3 weeks and peaking at 4 and 5 weeks, respectively (Thiesen et al., 2013). Post mortem diffusion tensor imaging (DTI), quantitative MTI (qMTI), and T1 /T2 measurement 6 weeks after cuprizone treatment were evaluated. Quantitative MTI metrics showed significant differences in the corpus callosum and external capsule of the cuprizone-fed mice, additionally FA (Fractional Anisotropy) was significantly lower and mean (MD), axial (AD), and radial diffusivity (RD) were significantly higher in the cuprizone-fed mice. Electron microscopy revealed strong cellular correlations with particular quantified MRI

results in the corpus callosum. T1 was correlated with the myelinated axon fraction; the bound pool fraction (f) was correlated with the myelin sheath fraction; and axial diffusivity was correlated with the non-myelinated cell fraction. Among calculated MRI metrics, *f* was the strongest indicator of myelin content, while the strongest indicators of changes in tissue structures were longitudinal relaxation rates and diffusivity measurements (MD, AD, RD, FA). The transfer rate between the bound (f) and free proton pools (k) and the bound pool fraction (f) itself were significantly decreased in the corpus callosum and external capsule. There was a significant correlation between (f) and the myelin sheath fraction emphasizing a relationship between a reduction in f and myelin loss (Thiessen et al., 2013).

In the study of Kim et al., (2015) a modified magnetization transfer indicator, MT asymmetry (MTA) was proposed allowing for more specific myelin imaging. In rat brain at 9.4 T MTA revealed strong signals in white matter and significantly lower signal in gray matter and muscle, suggesting higher specificity of MTA over MTR and as high sensitivity as MTR. Demyelination and remyelination were studied in rats following 4 weeks of cuprizone diet followed by remyelination for one week. The experimental results indicate that MTA can be a good indicator of myelin content. Additionally, MTA proved higher WM specificity than MTR (Kim et al., 2015). This imaging modality should be further explored.

MTR imaging – multiparametric approach.

To improve the effectiveness of MRI modalities in predicting/assessing myelination status, a multiparametric approach is often proposed. In such multimodal imaging study using cuprizone – induced demyelination, after 6 weeks of a diet T1W, T2W and MT imaging was performed to assess correlation of normalized MRI signal with electron microscopy evaluation results. On the basis of histological examination the g-ratio (the diameter of the axon divided by the fiber diameter), cellular density and the extent of astrogliosis were quantified. The results revealed considerable overlap between demyelinated and remyelinated animals as well as controls when considering normalized T2, T1 and MTR signals separately. However, when these

three metrics were taken into account simultaneously (using discriminant function analysis) they predicted myelin status in vivo with 95% accuracy when compared to electron microscopy tissue status (Merkler et al., 2005). In this experiment for normalized T1W signal and MTR maps, 3D FLASH sequence was used, resulting in a total acquisition time of 5 hours (Merkler et al., 2005).

In another experiment, a continuous decrease in MTR values was observed in following weeks of cuprizone diet in the corpus callosum and deep gray matter of mice fed 6 weeks with cuprizone. MTR values correlated to myelin loss detected by immunohistochemistry in both structures, but did not correlate to oligodendrocyte density, suggesting low specificity of this parameter for oligodendrocyte loss (Fjaer et al., 2013). In another study of this group, MTR was higher in control group than in EAE mouse, moreover, changes in MTR values did not correlate to myelin content, iron deposition and other disease tissue pathology parameters (Fjær et al, 2015).

Another example of a multiparametric approach is an experiment in which the dependence of T2W, MTR and DTI metrics was correlated to quantified electron microscopy results in the early stages of oligodendrocyte damage – weeks 2 and 3, following the cuprizone administration in mice (Friesen et al., 2024). Significant changes in normalized T2W signal intensity and non-significant changes in MTR were observed to correspond to early WM damage, whereas significant changes in both corresponded with full demyelination (Friesen et al., 2024). The strength of this experiment is that it correlates different MRI metrics (in vivo MTR, T1W, T2W, ex vivo DTI, qMTR, T1 and T2 maps) directly with electron microscopy findings, providing direct information about tissue structure while its weakness is the small number of animals per group (typically n=3). In this experiment very subtle changes of MTR correlated with non-myelinated content fraction but surprisingly MTR values did not correlate with other myelin damage related parameters (Friesen et al., 2024).

In a common marmoset EAE model, three different imaging modalities were evaluated: MTR imaging, PDW imaging and T1W-Gd imaging in terms of their sensitivity and specificity to remyelination detection. Out of these three methods

PDW imaging was very sensitive to remyelination – it detected 100% or remyelinated lesions with 90% specificity in 20 weeks long period following immunization. Based solely on PDW images investigators detected "early active lesions", "chronic lesions partially demyelinated" and "totally remyelinated lesions" with 90% specificity, and this status was then confirmed by histology. In this experiment MTR was less sensitive in lesion detection (82%) and also had lower specificity (Donadieu et al., 2023). The authors suspect that the lower MTR signal ability to correlate with remyelination may be the result of incomplete myelin sheath restoration or the effect of morphologically altered myelin (Donadieu et al., 2023).

Inhomogeneous Magnetization Transfer (ihMT) is a new imaging modality that results in new contrast, so called the dipolar order relaxation time (T_{1D}) weighting (Varma et al., 2017, Mannig et al., 2017). The source of this signal is tissue microstructure and slow motional processes including lipid membrane collective motions (Dufourc et al., 1992). It is suspected that the source of observed ihMT contrast is the mobility of methylene protons along the lipid chains in phospholipid bilayer in myelin (Varma et al., 2015; Manning et al., 2017). The potential of ihMT in myelin associated diseases has not yet been explored. However, in patients, it demonstrates better correlation with the Expanded Disability Status Scale (EDSS) score in comparison to MTR results detected in lesions (Zhang et al., 2020) and in NAWM (Van Obberghen et al., 2018). In the work of Zhang et al. (2020) no significant correlation was found between ihMTR values detected in NAWM and EDSS.

In ihMT imaging the manipulation with high-pass and band-pass T_{1D}-filters allows to adjust the relative contribution of long T_{1D}-components and short T_{1D}-components of the ihMT signal. This way, ihMT images can be weighted towards each of these components via variation in the switching time between RF pulses with opposite frequencies (Hertanu et al., 2023).

In the hypomyelinated white matter structures in the brain of shiverer mice, ihMT was shown to be highly sensitive to abnormal myelin sheath organization, resulting in up to a 40% ihMT signal change, showing high potential in the research of myelin repair processes (Lee et al., 2022). In cuprizone treated mice (a five-week treatment

followed by four weeks of remyelination) ihMT was a sensitive biomarker of de-/remyelination, being sensitive to spatial differences in the range myelination change in the corpus callosum. ihMT targeted towards long T1D components had higher sensitivity showing better correlation to myelin histology results (Hertanu et al.,2023).

Another imaging option using MTR imaging is an application of Ultrashort echo time (UTE) MRI for MTR evaluation. This experimental approach seems to be more sensitive for demyelination detection with a potential to improve lesion detection as it is a more direct imaging of lipids and myelin sheaths. Two pulse sequences combining magnetization transfer (MT) with 3D UTE ("UTE-MT", TE = 76 μs) and with short TE gradient echo ("STE-MT", TE = 3000 μs) were used to evaluate spatial and temporal changes in brain myelin content in the cuprizone mouse model on a clinical 7 T scanner. Both measures significantly decreased in most white matter and grey matter regions, but only UTE has detected cortical change. After remyelination in subcortical and cortical areas, UTE-MTR values remained lower than baseline values thus detecting long lasting changes following demyelination. Also UTE derived MTR had the strongest correlation with histological markers of myelination (Guglielmetti et al., 2020).

In an interesting study, inversion recovery (IR) UTE sequence was proved to be helpful in myelin status differentiation in cuprizone treated rodents (Piedzia et al., 2014).

The research allowing for manipulation with the amount of inflammation in EAE model revealed in NAWM of guinea pigs that MTR is sensitive to physiological changes induced by inflammation. That notion supports the hypothesis that pathologic features other than demyelination may be important source of MTR signal change (Gareau et al., 2000). Human study has also found a linear relationship between water content and MTR signal, while no close relationship was found between myelin water content and MTR signal supporting the hypothesis that inflammation and edema influence MTR values (Vavasour et al., 2011). That notion is confirmed by the fact that MS patients showed transient changes in brain size and

MTR signal related to a decrease in brain water following corticosteroids treatment (Fox et al., 2005). In MS lesions, MTR signal contribution from edema, inflammation and changes in extracellular water is assumed to contribute to the final MTR signal (Fox et al., 2005). In a murine spinal cord following lysolecithine injection, the MTR signal shoved no sensitivity to early demyelination and this result was explained as the reflection of the myelin debris presence in the early demyelination stage (McCreary et al., 2009). In the study of the EAE rat model, MTR decreased before the histological appearance of demyelination. That phenomenon was explained as being related to early inflammation events in the lesion formation process (Serres et al., 2009).

In the application of MTR for myelination monitoring a major limitation is that while a change in myelin will cause a change in MT, a change in MT is not necessarily caused by a change in myelination. Changes in other tissue components such as axons and glia, as well as changes in water content due to inflammation or edema will result in changes in MT (Mottershead et al.,2003, Vavasour et al., 2011). Newer magnetization transfer related methods, such as inhomogeneous magnetization transfer (ihMT) and asymmetric magnetization transfer (AMT) are promising candidates for more specific myelin detection (Laule and Moore, 2018, Alsop et al., 2023).

In general, MTR is decreased in MS and in animal models of MS. However, the results received from the research in animals are slightly inconsistent across different studies (Nathoo et al., 2014, Jelescu et al., 2016. Friesen et al., 2024) suggesting MT sensitivity but not specificity for myelination status. In post mortem evaluation of different types of lesions (chronic demyelinated vs remyelinated lesions) in MS brains, MTR imaging showed strong influence of components other than myelin and a high dependency on tissue storage duration (Wiggermann et al., 2023).

While MTR imaging does not require a long acquisition time, it has some limitations as it visualizes myelin indirectly through restricted proton pool motion, and is unable to differentiate between myelin and myelin debris. Also edema and inflammation are influencing the MTR signal further increasing its lack of specificity.

A study with cuprizone-induced demyelination, which correlated myelin biomarkers with electron–microscopy, has revealed relatively poor myelin specificity of MTR imaging (Jelescu et al., 2016, Merkler et al., 2005, Friessen et al., 2024), especially as compared to other advanced imaging modality - diffusional kurtosis imaging (DKI), (Jelescu et al., 2016). New MTR techniques, in particular inhomogeneous magnetization transfer (ihMT) holds a promise to improve this method specificity to myelin status.

Diffusion – based imaging modalities: DTI, DKI and high b-value q-space imaging.

Another approach to detect myelin status in MS lesions utilizes diffusion based imaging modalities. This kind of imaging is probing the random motion of water molecules (diffusion) and relating that phenomenon to the structural barriers present in healthy tissues, to reveal microstructural pathology (Figueriedo et al., 2011). Diffusion imaging is not included in standard clinical imaging protocols but can be useful in MS monitoring (Filippi and Rocca, 2011). In diffusion weighted imaging the results depend on the biophysical model used to categorize the imaging data. The two most extensively used are Diffusion Tensor Imaging (DTI) and neurite orientation dispersion and density imaging (NODDI) imaging. DTI had been frequently used in MS research while NODDI imaging is becoming an important tool of research due to its novelty and multiplicity of tissue derived parametrization. NODDI also overcomes some of the DTI limitations.

In conventional diffusion tensor imaging (DTI), diffusion distribution of water molecules is described as a 2nd-order three-dimensional (3D) diffusivity tensor. It assumes that diffusion occurs in a free and unrestricted environment with a Gaussian distribution of diffusion displacement. As a consequence, that diffusion weighted (DW) signal decays with the diffusion factor (b-value) monoexponentially. In biological tissue, complex cellular microstructures influence diffusion, making it a highly restricted process. Non-monoexponential decays are observed in both WM

and GM. As a result, DTI quantitation is b-value dependent and DTI fails to fully utilize the diffusion measurements that are inherent to tissue microstructure.

DTI provides information on the preferred direction of the water displacement, by investigating the structure of the water diffusion distribution: it assumes that the motion of water molecules follows a 3D Gaussian distribution and can be characterized by a diffusion tensor in each voxel. The metrics that result from this model are mean diffusivity (MD also referred as Apparent Diffusion Coefficient, ADC), fractional anisotropy (FA), radial diffusivity (RD), and axial diffusivity (AD).

A comparative analysis of MRI and histopathology results revealed a high correlation between the DTI changes and axonal count in WM lesions and NAWM which may be related to the level of disability (Schmierer et al., 2007, Preziosa et al., 2011). Despite the DTI sensitivity, the lack of its specificity in detecting microstructural changes in WM is the main weakness when this imaging modality is applied for lesion evaluation. In particular, DTI results are affected by the orientation dispersion of fibers leading often to misinterpretation, especially when two or more different tissues exist in a single voxel (Schneider et al., 2017). Some recent work pointed out the possibility of further improvement of DWI metrics when b-matrix spatial distribution correction (BSD – DTI) is applied, to correct errors induced by local gradient fields inhomogeneities (Krzyzak et al., 2024, Krzyzak et al., 2025). Application of such a correction, may improve accuracy of DTI metrics resulting in specificity increase. This approach needs further evaluation in an animal models, where due to higher field strength, local inhomogeneities may be more profound.

DKI is a higher order extension of DTI because it quantifies the deviation from Gaussian diffusion in the tissues, providing information about tissue heterogeneity (Jensen et al., 2005). DKI combines a 2nd-order 3D diffusivity tensor obtained using conventional DTI with a 4th-order 3D kurtosis tensor. Since kurtosis is a measure of the deviation of the diffusion displacement profile from a Gaussian distribution, that technique allows to quantify the degree of diffusion restriction in particular tissue without making biophysical assumptions.

On the basis of DKI, the white matter tract integrity (WMTI) model was developed. It allows to characterize the intra- and extra-axonal compartments in WM fibres, based on the measurement of diffusion and kurtosis tensors (Fieremans et al., 2011; Fieremans et al., 2010).

In the WMTI model, the intra-axonal space is modelled as a collection of sticks (cylinders with negligible radius) while the extra-axonal space is assumed to be a Gaussian anisotropic compartment. Exchange between the intra- and extra-axonal spaces is assumed nonexistent. The water MR signal originates from the collective intra-axonal and extra-axonal spaces. The model derives an estimate of the axonal water fraction (AWF), axonal diffusivity (Da), and extra-axonal parallel ($D_{e,\parallel}$) and radial ($D_{e,\perp}$) diffusivities. The WMTI model is based on two assumptions. First, WM tracts are highly aligned. Second, Da is assumed to be smaller than or equal to $D_{e,\parallel}$ (rather than $Da \geq D_{e,\parallel}$). This second assumption affects the values of Da and and $D_{e,\parallel}$, while the AWF and $D_{e,\perp}$ values are not affected. The extraction of WMTI metrics can be made directly from the DKI data (Fieremans et al., 2011; Fieremans et al., 2010).

WMTI metrics may more easily correlate to tissue damage than empirical DTI because of their higher specificity to the underlying tissue architecture and disease mechanisms. Extra axonal radial diffusivity ($D_{e,\perp}$) can be particularly sensitive to demyelination and g-ratio change, while AWF could be more sensitive to axonal loss and/or patchy demyelination (Novikov and Fieremans, 2012). Indeed, a decrease in AWF does not necessarily imply axonal loss but can also be an indirect effect of an increase in the extra-axonal volume fraction following demyelination. Simultaneous decreases in $D_{e,\perp}$ and $D_{e,\parallel}$ could be a result of increased extra-axonal density caused by inflammation, astrocytosis and gliosis. A decrease of Da is an indicative of acute intra-axonal injury (Grossman et al., 2015; Hui et al., 2012). Based on these features, WMTI has so far provided an insightful characterization of white matter changes in many pathological WM states including multiple sclerosis (Fieremans et al., 2012) and cuprizone – induced demyelination (Falangola et al., 2014).

First group which establish sensitivity of DKI in demyelination detection in comparison to DTI were Falangola et al., (2014). In chronic cuprizone administration

in rats (10 weeks) the diffusional kurtosis (DK) and WM modelling metrics were found to provide additional information that enhances the sensitivity to detect the morphological heterogeneity in the rostral segment of the corpus callosum. Axonal water fraction, radial kurtosis and mean kurtosis showed the highest sensitivity to demyelination (Falangola et al., 2014).

In the mouse corpus callosum, following acute cuprizone administration for six weeks, a significant decrease in AWF and mild changes in extra-axonal radial diffusivity were detected (Jelescu et al., 2016). Chronic demyelination induced by twelve weeks of cuprizone administration resulted in a more pronounced decrease in extra-axonal radial diffusivity. This is consistent with the more severe demyelination in histological evaluation. The axonal water fraction (AWF) correlated significantly with the AWF quantified by EM but not with the g-ratio, while the extra-axonal radial diffusivity correlated with the g-ratio but not with the EM – derived AWF (Jelescu et al., 2016). In this experiment T_2 values had the largest standardized difference between cuprizone and controls, followed by AWF (derived by DKI) and RD. The differences between acute and chronic cuprizone administration were only observed ~~only~~ in terms of RD and T_2. MTR did not correlate with all but one EM-derived axonal metrics. All analyses were performed on a single sagittal image with the corpus callosum for MTR, T2W and DKI imaging to maintain 'a reasonable acquisition time' (Jelescu et al., 2016).

In the cuprizone mouse model the temporal evolution of normalized T2 changes, diffusion tensor metrics and diffusion kurtosis tensor together with WMTI metrics were analyzed in GM and in WM three weeks (moderate demyelination) and six weeks (severe demyelination) of continuous cuprizone intoxication (Guglielmetti et al., 2016). In cortical alterations, DT-derived metrics were unable to detect cuprizone induced changes while the mean kurtosis (MK) and radial kurtosis (RK) decreased under cuprizone administration in both moderate and severe demyelination, as compared to age-matched controls. The values of both kurtosis metrics returned to control levels at the end of the recovery period. In the regions of most prominent WM changes (in the splenium and body of the corpus callosum) WMDT metrics (MD, RD) showed sensitivity to moderate and severe changes with the same

evolution. After three weeks of intoxication both metrics decreased and then elevated following six weeks of cuprizone. At the level of less demyelinated areas (the genu of the corpus callosum) DTI derived metrics didn't show changes at any time point. In this experiment MK, RK and AWF were the most sensitive metrics for the detecting cuprizone induced changes in the genu of the corpus callosum, a region less affected by cuprizone administration. WMTI-derived metrics showed the ability to distinguish between the severity of demyelination. The acquisition time of this experiment was about four hours (Guglielmetti et al., 2016).

In conclusion DKI partially resolves-the problem of long scanning times apparent in q-Space Imaging (qSI). It allows the calculation of kurtosis values, not the entire PDF itself, thus different b -value measurement can be reduced by up to six steps. As a result, the acquisition time is reduced. On the other hand, DKI suffers from the omission of high b-values, which may compromise its specificity to myelin signals (Cohen and Asaf., 2002), because the diffusion-related signal decay curve in WM is multiexponential and the accuracy of the PDF depends upon data with high *b*-values (~10,000 s/mm2), (Cohen et al.,2002). Extracting WMTI metrics directly from (DKI) provides a better description of chronically demyelinated lesions. (Falangola et al., 2014 Jelescu et al., 2016, Guglielmetti et al., 2016).

High-b-value q-space imaging could be a fruitful alternative for DKI. It is an advanced diffusion MRI modality that has been proved be sensitive to demyelination and WM changes in animal models (Assaf et al., 2000, Cohen and Assaf , 2002). The q-space method measures the displacement distribution profile of water molecules in the tissue and quantifies it by its width (displacement index) or height (probability index) (Assaf et al., 2005). Using the displacement distribution profile, it is possible to distinguish between free and restricted modes of diffusion, if a sufficiently long diffusion time and a high b-value are used (Cory and Garroway, 1990). The influence of axonal content (the neurofilaments), myelin layers and also other factors might restrict water motion (Assaf and Cohen, 2000). In this imaging modality contribution of restricted diffusion components in WM, which may reflect axonal damage more precisely, is emphasized. That method was successfully used in clinical scanners to detect a marked increase in the apparent displacement index and a reduction in the

apparent probability index in the areas of MS lesions. These results were interpreted as an effect of demyelination on tissue disintegration, which was present in WM lesions and to a lesser extent, in NAWM. For imaging in this modality b-values up to 14000 s/mm2 were used (Assaf et al., 2002).

To address the problem of the nonspecific MRI appearance of WM lesions which does not reflect its myelination and functional status so called q-space Myelin Map (qMM) imaging was proposed. The authors claim that this method, allows for a more reliable mapping of the compartmentalization of water within myelin sheets structures (Nakhara et al., 2019). In this imaging option, the introduction of high b-values, which are essential for myelin signal acquisition was proposed, resulting in qMM. Compared to q-space imaging, qMM uses fewer but higher b-values, resulting in increased myelin specificity (Fujiyoshi et al., 2016). The principal difference between the myelin map and full-scale qSI is the number of b-value steps, whereas the difference between the qMM and DKI is the range of b-values. Additionally, the myelin map imaging uses a heat map based on standardized kurtosis values, making it easier to compare data between individuals within the same species (Kitagawa et al., 2024). qMM imaging can detect the movement of protons with a resolution of less than an axonal diameter (10 μm), so it should be able to detect myelin sheaths in a scanned area and remain insensitive to myelin debris (Fujiyoshi et al., 2016). Furthermore, qMM could be acquired within 10 min using an ordinal 3-T MR scanner, in a clinical setting.

In qMM imaging a reduced number of high b-values (9 steps, up to 10000 s/mm^2) allows for reconstruction of heat map of the standardized kurtosis values (reconstructed on the basis of calculated normalized leptokurtic diffusion - NLD). The detailed description of the calculation is presented in Fujiyoshi et al., (2016). Such experimental design demonstrates its sensitivity to visualise remyelination in the process of MS progression inhibition. For patient with the observed functional improvement after the treatment, qMM allows to detect changes in patient's myelin signal from lesions, which had been appearing constantly bright on T_2-weighted images (Fujiyoshi et al., 2016). This imaging modality was proven to be useful in the assessment of focal demyelination in spinal cord of common marmosets following

injection of lysophatidylcholine. In this experiment, qMM shown signal disappearance and reappearance as a result of consecutive demyelination and remyelination, which was confirmed by histological staining and electron microscopy examination. The study was performed at 7 tesla preclinical MRI scanner. In healthy volunteers, in comparison to FA map and DTI map, myelin map shown a significantly higher contrast in detecting myelin signals, not only in deep white matter, such as the corpus callosum, but also in the cortical WM suggesting that the myelin map has higher sensitivity than FA map or other DTI maps at detecting myelin signals in the human brain (Fujiyoshi et al., 2016).

That approach started to be explored in clinical follow up, especially in the clinical trials of a potential medications promoting the remyelination. In such study 48 patients with relapsing remitting MS received 4 different medications: in 46% of them remyelination was detected using qMM imaging. Additionally, two recovery promoting factors were identified based on correlation of qMM results with particular type of medication: younger age (in case of natalizumab) and female sex (in case of dimethyl fumarate) correlated positively with remyelinating treatment outcome detected by qMM imaging (Kitagawa et al.,2024, see Fig. 6).

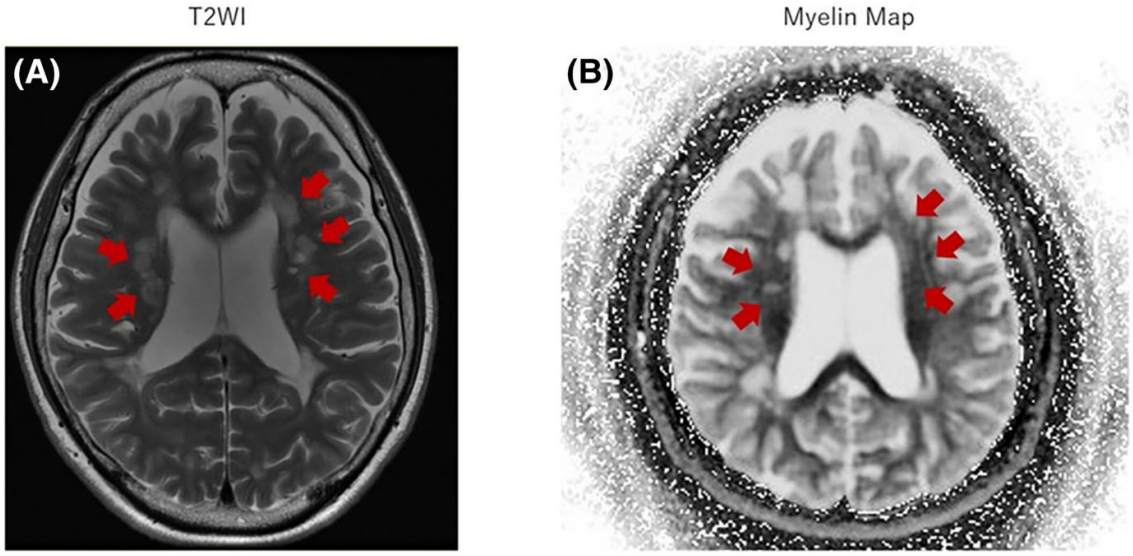

Fig. 6. T2-weighted image (T2WI) and *q*-space Myelin Map (qMM) in a brain of a patient with relapsing–remitting multiple sclerosis (a 60 year old man) are shown. Red arrows indicate multiple sclerosis lesions (i.e. "T2-lesions") . In qMM image

positive myelin signal is suggesting remyelination of a lesion while T2W signal remains unchanged following treatment. Probability of remyelination is also confirmed by neurological improvement. Reprinted without changes with permission from Kitagawa et al., 2024, doi: 10.1111/cen3.12796, https://onlinelibrary.wiley.com/doi/10.1111/cen3.12796, https://creativecommons.org/licenses/by-nc/4.0/

Imaging procedure allowing for calculation of qMM detected MRI tissue appearance suggesting remyelination in 6 (out of total 8) fingolimod – treated patients (Tanikawa et al., 2017). Fingolimod (FTY) is a disease modifying drug, known as a successful inhibitor of disability progression in 30% of MS patients (Kappos et al., 2016). For qMM a pulsed-field gradient spin-echo (PGSE) sequence was performed along 12 gradient directions, with 9 b-values (range 0–10,000s/mm^2). The lesions were considered a newly evolving demyelinating, when on qMM 50% signal loss was registered in a lesion as compared to adjacent NAWM signal. When the signal increased by 50% of its initial value, the lesion was considered remyelinated. The myelin map was recorded within 10 min allowing for calculation of remyelination and newly evolving demyelinating lesions. The results showed an increased qMM signal (suggesting remyelination) together with improved disability in 6 patients (Tanikawa et al., 2017).

Another option, based on a results received from the optimized *q*-space diffusion imaging using high b-values is calculation of the Normalized Leptokurtic Diffusion (NLD) map. This imaging option presents very important advantage over Diffusion Kurtosis Imaging (DKI) from which it was derived, as it allows for the use of high *b*-values with concomitant limitation of the number of acquisition steps to nine. That makes possible acquisition of a high-spatial-resolution images relatively quickly.

In the retrospective analysis of a Normalized Leptokurtic Diffusion (NLD) index in around one hundred patients with different stage of MS and different EDSS indexes, worse EDSS scores were significantly associated with a lower NLD index in the Corpus Callosum (CC) and a lower non-lesional WM-NLD index. Both NLD indexes (in the CC and in a non-lesional WM) were significantly lower in the

moderate/severe MS compared to mild MS group (severe group: EDSS≥4, mild group: EDSS <4). Additionally, normalized leptokurtic diffusion index correlates with cognitive impairment evaluated in the mental tests (Motegi et al., 2024). Moreover, NLD index value was an indicator of a MS type. A decrease in NLD indexes was observed in a progressive MS, for particular WM structures including non lesion WM as compared to relapsing-remitting MS. This way the NLD index was correlated to the clinical status of MS patients.

In summary, several metrics acquired from diffusion tensor images have been linked to myelin status in MS in patients as well in animal models of de-/re-myelination. The perpendicular component of the diffusion tensor (radial diffusivity) is related to myelination status in animal models, however the presence of edema and/or crossing fibers can compromise DTI metrics. More sophisticated diffusion modeling and analysis approaches are now emerging including neurite orientation dispersion and density imaging (NODDI) and diffusion basis spectrum imaging (DBSI) providing more specific assessment of tissue components, including myelin (Schilling et al., 2017, Wang et al., 2014, Sommer et al., 2022) in MS and in animal models. Among different imaging modalities ultrashort echo time (UTE) measures signal from non-water sources of hydrogen, including the lipids and proteins that make up myelin (Robson et al., 2003), which seems to be important and promising tool for future research. Among the advanced MRI derived metrics, qMM (NLD index), DKI and MWF demonstrated the highest specificity toward myelination status detection, being promising MRI modalities for future experimental trials and clinical applications.

Discussion

Conventional magnetic resonance imaging metrics such as T_2, T_1, T_1-Gd have limited ability to differentiate unmyelinated and remyelinated lesions, since they proved sensitivity but not specificity. The lack of correlation between magnetic resonance imaging results and existent tissue pathology is called a ‘clinico-radiological paradox' (Barkhof, 2002). Advanced MRI sequences based on magnetization transfer ratio

(MTR), diffusion kurtosis imaging (DKI) and myelin water fraction (MWF) and also diffusion tensor imaging (DTI) have been used to evaluate remyelination in clinical trials and in animal models of demyelination. Among them DKI along with the white matter tract integrity (WMTI) modelling, have proved highest specificity. That specificity was even higher when more recently developed high b-value q-space imaging modalities were applied. Among them a high b-value q-space myelin map (qMM) with calculated Normalized Leptokurtic Diffusion (NLD) index has been applied in an experimental and exploratory clinical studies, showing most promising results in terms of myelin specificity.

There are three strategies to overcome MRI limitations in visualizing myelin pathology: more advanced hardware strategies – particularly higher magnetic field strength scanners, which can result in sensitivity increase, automatic post imaging voxelwise techniques which help to visualize and quantify myelin changes and the development and application of new imaging modalities, helping visualize a pathological changes not visible with the application of traditional techniques. The last strategy was reviewed here in terms of comparing conventional MRI techniques results aimed at myelination status evaluation (T1W, T2W, PDW, T1-Gd) with more sophisticated methods such as MTR, DTI, DKI, and modalities emerged from high b-value q-space imaging. Out of discussed here, the newly emerging imaging modalities qMM, DKI and MWF showed higher specificity to myelin status changes, holding a promise that they may help to resolve 'clinico-radiological paradox' in future research and diagnosis.

References

1. Absinta M, Sati P, Reich DS. Advanced MRI and staging of multiple sclerosis lesions. Nat Rev Neurol. 2016 Jun;12(6):358-68. doi: 10.1038/nrneurol.2016.59.
2. Acs P, Selak MA, Komoly S, Kalman B. Distribution of oligodendrocyte loss and mitochondrial toxicity in the cuprizone-induced experimental demyelination model. J Neuroimmunol. 2013 Sep 15;262(1-2):128-31. doi: 10.1016/j.jneuroim.2013.06.012.
3. Adamo AM, Paez PM, Escobar Cabrera OE, Wolfson M, Franco PG, Pasquini JM, Soto EF. Remyelination after cuprizone-induced demyelination in the rat is

stimulated by apotransferrin. Exp Neurol. 2006 Apr;198(2):519-29. doi: 10.1016/j.expneurol.2005.12.027.

4. Agrawal SM, Silva C, Tourtellotte WW, Yong VW. EMMPRIN: a novel regulator of leukocyte transmigration into the CNS in multiple sclerosis and experimental autoimmune encephalomyelitis. J Neurosci. 2011 Jan 12;31(2):669-77. doi: 10.1523/JNEUROSCI.3659-10.2011.
5. Aktas O, Smorodchenko A, Brocke S, Infante-Duarte C, Schulze Topphoff U, Vogt J, Prozorovski T, Meier S, Osmanova V, Pohl E, Bechmann I, Nitsch R, Zipp F. Neuronal damage in autoimmune neuroinflammation mediated by the death ligand TRAIL. Neuron. 2005 May 5;46(3):421-32. doi: 10.1016/j.neuron.2005.03.018.
6. Alsop DC, Ercan E, Girard OM, Mackay AL, Michal CA, Varma G, Vinogradov E, Duhamel G. Inhomogeneous magnetization transfer imaging: Concepts and directions for further development. NMR Biomed. 2023 Jun;36(6):e4808. doi: 10.1002/nbm.4808.
7. Assaf Y, Ben-Bashat D, Chapman J, Peled S, Biton IE, Kafri M, Segev Y, Hendler T, Korczyn AD, Graif M, Cohen Y. High b-value q-space analyzed diffusion-weighted MRI: application to multiple sclerosis. Magn Reson Med. 2002 Jan;47(1):115-26. doi: 10.1002/mrm.10040.
8. Assaf Y, Chapman J, Ben-Bashat D, Hendler T, Segev Y, Korczyn AD, Graif M, Cohen Y. White matter changes in multiple sclerosis: correlation of q-space diffusion MRI and 1H MRS. Magn Reson Imaging. 2005 Jul;23(6):703-10. doi: 10.1016/j.mri.2005.04.008.
9. Assaf Y, Cohen Y. Assignment of the water slow-diffusing component in the central nervous system using q-space diffusion MRS: implications for fiber tract imaging. Magn Reson Med. 2000 Feb;43(2):191-9. doi: 10.1002/(sici)1522-2594(200002)43:2<191::aid-mrm5>3.0.co;2-b.
10. Assaf Y, Mayk A, Cohen Y. Displacement imaging of spinal cord using q-space diffusion-weighted MRI. Magn Reson Med. 2000 Nov;44(5):713-22. doi: 10.1002/1522-2594(200011)44:5<713::aid-mrm9>3.0.co;2-6.
11. Barkhof F, Bruck W, De Groot CJ, Bergers E, Hulshof S, Geurts J, Polman CH, van der Valk P. Remyelinated lesions in multiple sclerosis: magnetic resonance image appearance. Arch Neurol. 2003 Aug;60(8):1073-81. doi: 10.1001/archneur.60.8.1073.
12. Battefeld A, Klooster J, Kole MH. Myelinating satellite oligodendrocytes are integrated in a glial syncytium constraining neuronal high-frequency activity. Nat Commun. 2016 May 10;7:11298. doi: 10.1038/ncomms11298.
13. Baxi EG, DeBruin J, Jin J, Strasburger HJ, Smith MD, Orthmann-Murphy JL, Schott JT, Fairchild AN, Bergles DE, Calabresi PA. Lineage tracing reveals dynamic changes in oligodendrocyte precursor cells following cuprizone-induced demyelination. Glia. 2017 Dec;65(12):2087-2098. doi: 10.1002/glia.23229.

14. Bergamino C, Hoey S, Waller K, Skelly C. Comparison of T1wFLAIR and T1wTSE sequences in imaging the brain of small animals using high-field MRI. Ir Vet J. 2019 Jul 6;72:6. doi: 10.1186/s13620-019-0145-5.
15. Billiet T, Vandenbulcke M, Mädler B, Peeters R, Dhollander T, Zhang H, Deprez S, Van den Bergh BR, Sunaert S, Emsell L. Age-related microstructural differences quantified using myelin water imaging and advanced diffusion MRI. Neurobiol Aging. 2015 Jun;36(6):2107-21. doi: 10.1016/j.neurobiolaging.2015.02.029.
16. Bou Fakhredin R, Saade C, Kerek R, El-Jamal L, Khoury SJ, El-Merhi F. Imaging in multiple sclerosis: A new spin on lesions. J Med Imaging Radiat Oncol. 2016 Oct;60(5):577-586. doi: 10.1111/1754-9485.12498.
17. Boutitah-Benyaich I, Eixarch H, Villacieros-Álvarez J, Hervera A, Cobo-Calvo Á, Montalban X, Espejo C. Multiple sclerosis: molecular pathogenesis and therapeutic intervention. Signal Transduct Target Ther. 2025 Oct 2;10(1):324. doi: 10.1038/s41392-025-02415-4.
18. Brownlee WJ, Hardy TA, Fazekas F, Miller DH. Diagnosis of multiple sclerosis: progress and challenges. Lancet. 2017 Apr 1;389(10076):1336-1346. doi: 10.1016/S0140-6736(16)30959-X.
19. Buttigieg E, Scheller A, El Waly B, Kirchhoff F, Debarbieux F. Contribution of Intravital Neuroimaging to Study Animal Models of Multiple Sclerosis. Neurotherapeutics. 2023 Jan;20(1):22-38. doi: 10.1007/s13311-022-01324-6.
20. Campi A, Filippi M, Comi G, Scotti G, Gerevini S, Dousset V. Magnetisation transfer ratios of contrast-enhancing and nonenhancing lesions in multiple sclerosis. Neuroradiology. 1996 Feb;38(2):115-9. doi: 10.1007/BF00604792.
21. Chang A, Staugaitis SM, Dutta R, Batt CE, Easley KE, Chomyk AM, Yong VW, Fox RJ, Kidd GJ, Trapp BD. Cortical remyelination: a new target for repair therapies in multiple sclerosis. Ann Neurol. 2012 Dec;72(6):918-26. doi: 10.1002/ana.23693.
22. Cohen Y, Assaf Y. High b-value q-space analyzed diffusion-weighted MRS and MRI in neuronal tissues - a technical review. NMR Biomed. 2002 Nov-Dec;15(7-8):516-42. doi: 10.1002/nbm.778.
23. Constantinescu CS, Farooqi N, O'Brien K, Gran B. Experimental autoimmune encephalomyelitis (EAE) as a model for multiple sclerosis (MS). Br J Pharmacol. 2011 Oct;164(4):1079-106. doi: 10.1111/j.1476-5381.2011.01302.x.
24. Cory DG, Garroway AN. Measurement of translational displacement probabilities by NMR: an indicator of compartmentation. Magn Reson Med. 1990 Jun;14(3):435-44. doi: 10.1002/mrm.1910140303.
25. Cotton F, Weiner HL, Jolesz FA, Guttmann CR. MRI contrast uptake in new lesions in relapsing-remitting MS followed at weekly intervals. Neurology. 2003 Feb 25;60(4):640-6. doi: 10.1212/01.wnl.0000046587.83503.1e.

26. Cree BAC, Arnold DL, Chataway J, Chitnis T, Fox RJ, Pozo Ramajo A, Murphy N, Lassmann H. Secondary Progressive Multiple Sclerosis: New Insights. Neurology. 2021 Aug 24;97(8):378-388. doi: 10.1212/WNL.0000000000012323.
27. De Coene B, Hajnal JV, Gatehouse P, Longmore DB, White SJ, Oatridge A, Pennock JM, Young IR, Bydder GM. MR of the brain using fluid-attenuated inversion recovery (FLAIR) pulse sequences. AJNR Am J Neuroradiol. 1992 Nov-Dec;13(6):1555-64.
28. Deloire-Grassin MS, Brochet B, Quesson B, Delalande C, Dousset V, Canioni P, Petry KG. In vivo evaluation of remyelination in rat brain by magnetization transfer imaging. J Neurol Sci. 2000 Sep 1;178(1):10-6. doi: 10.1016/s0022-510x(00)00331-2.
29. DePaula-Silva AB, Hanak TJ, Libbey JE, Fujinami RS. Theiler's murine encephalomyelitis virus infection of SJL/J and C57BL/6J mice: Models for multiple sclerosis and epilepsy. J Neuroimmunol. 2017 Jul 15;308:30-42. doi: 10.1016/j.jneuroim.2017.02.012.
30. Donadieu M, Lee NJ, Gaitán MI, Ha SK, Luciano NJ, Roy S, Ineichen B, Leibovitch EC, Yen CC, Pham DL, Silva AC, Johnson M, Jacobson S, Sati P, Reich DS. In vivo MRI is sensitive to remyelination in a nonhuman primate model of multiple sclerosis. Elife. 2023 Apr 21;12:e73786. doi: 10.7554/eLife.73786.
31. Dousset V, Brochet B, Vital A, Gross C, Benazzouz A, Boullerne A, Bidabe AM, Gin AM, Caille JM. Lysolecithin-induced demyelination in primates: preliminary in vivo study with MR and magnetization transfer. AJNR Am J Neuroradiol. 1995 Feb;16(2):225-31. PMID: 7726066;
32. Dousset V, Grossman RI, Ramer KN, Schnall MD, Young LH, Gonzalez-Scarano F, Lavi E, Cohen JA. Experimental allergic encephalomyelitis and multiple sclerosis: lesion characterization with magnetization transfer imaging. Radiology. 1992 Feb;182(2):483-91. doi: 10.1148/radiology.182.2.1732968.
33. Dufourc EJ, Mayer C, Stohrer J, Althoff G, Kothe G. Dynamics of phosphate head groups in biomembranes. Comprehensive analysis using phosphorus-31 nuclear magnetic resonance lineshape and relaxation time measurements. Biophys J. 1992 Jan;61(1):42-57. doi: 10.1016/S0006-3495(92)81814-3.
34. Duncan ID, Brower A, Kondo Y, Curlee JF Jr, Schultz RD. Extensive remyelination of the CNS leads to functional recovery. Proc Natl Acad Sci USA. 2009 Apr 21;106(16):6832-6. doi: 10.1073/pnas.0812500106.
35. Enzinger C, Pinter D, Rocca MA, De Luca J, Sastre-Garriga J, Audoin B, Filippi M. Longitudinal fMRI studies: Exploring brain plasticity and repair in MS. Mult Scler. 2016 Mar;22(3):269-78. doi: 10.1177/1352458515619781.
36. Falangola MF, Guilfoyle DN, Tabesh A, Hui ES, Nie X, Jensen JH, Gerum SV, Hu C, LaFrancois J, Collins HR, Helpern JA. Histological correlation of diffusional kurtosis and white matter modeling metrics in cuprizone-induced corpus callosum demyelination. NMR Biomed. 2014;27:948–957. doi: 10.1002/nbm.3140.

37. de Figueiredo EH, Borgonovi AF, Doring TM. Basic concepts of MR imaging, diffusion MR imaging, and diffusion tensor imaging. Magn Reson Imaging Clin N Am. 2011 Feb;19(1):1-22. doi: 10.1016/j.mric.2010.10.005.
38. Fieremans E, Jensen JH, Helpern JA. White matter characterization with diffusional kurtosis imaging. Neuroimage. 2011 Sep 1;58(1):177-88. doi: 10.1016/j.neuroimage.2011.06.006.
39. Fieremans E, Novikov DS, Jensen JH, Helpern JA. Monte Carlo study of a two-compartment exchange model of diffusion. NMR Biomed. 2010 Aug;23(7):711-24. doi: 10.1002/nbm.1577.
40. Filippi M, Brück W, Chard D, Fazekas F, Geurts JJG, Enzinger C, Hametner S, Kuhlmann T, Preziosa P, Rovira À, Schmierer K, Stadelmann C, Rocca MA; Attendees of the Correlation between Pathological and MRI findings in MS workshop. Association between pathological and MRI findings in multiple sclerosis. Lancet Neurol. 2019 Feb;18(2):198-210. doi: 10.1016/S1474-4422(18)30451-4.
41. Filippi M, Rocca MA, Ciccarelli O, De Stefano N, Evangelou N, Kappos L, Rovira A, Sastre-Garriga J, Tintorè M, Frederiksen JL, Gasperini C, Palace J, Reich DS, Banwell B, Montalban X, Barkhof F; MAGNIMS Study Group. MRI criteria for the diagnosis of multiple sclerosis: MAGNIMS consensus guidelines. Lancet Neurol. 2016 Mar;15(3):292-303. doi: 10.1016/S1474-4422(15)00393-2.
42. Fischbach F, Nedelcu J, Leopold P, Zhan J, Clarner T, Nellessen L, Beißel C, van Heuvel Y, Goswami A, Weis J, Denecke B, Schmitz C, Hochstrasser T, Nyamoya S, Victor M, Beyer C, Kipp M. Cuprizone-induced graded oligodendrocyte vulnerability is regulated by the transcription factor DNA damage-inducible transcript 3. Glia. 2019 Feb;67(2):263-276. doi: 10.1002/glia.23538.
43. Fjær S, Bø L, Lundervold A, Myhr KM, Pavlin T, Torkildsen O, Wergeland S. Deep gray matter demyelination detected by magnetization transfer ratio in the cuprizone model. PLoS One. 2013 Dec 30;8(12):e84162. doi: 10.1371/journal.pone.0084162.
44. Fjær S, Bø L, Myhr KM, Torkildsen Ø, Wergeland S. Magnetization transfer ratio does not correlate to myelin content in the brain in the MOG-EAE mouse model. Neurochem Int. 2015 Apr-May;83-84:28-40. doi: 10.1016/j.neuint.2015.02.006.
45. Fox RJ, Fisher E, Tkach J, Lee JC, Cohen JA, Rudick RA. Brain atrophy and magnetization transfer ratio following methylprednisolone in multiple sclerosis: short-term changes and long-term implications. Mult Scler. 2005 Apr;11(2):140-5. doi: 10.1191/1352458505ms1142oa.
46. Friesen E, Sheft M, Hari K, Palmer V, Zhu S, Herrera S, Buist R, Jiang D, Li XM, Del Bigio MR, Thiessen JD, Martin M. Quantitative Analysis of Early White Matter Damage in Cuprizone Mouse Model of Demyelination Using 7.0 T MRI Multiparametric Approach. ASN Neuro. 2024;16(1):2404366. doi: 10.1080/17590914.2024.2404366.

47. Fujiyoshi K, Hikishima K, Nakahara J, Tsuji O, Hata J, Konomi T, Nagai T, Shibata S, Kaneko S, Iwanami A, Momoshima S, Takahashi S, Jinzaki M, Suzuki N, Toyama Y, Nakamura M, Okano H. Application of q-Space Diffusion MRI for the Visualization of White Matter. J Neurosci. 2016 Mar 2;36(9):2796-808. doi: 10.1523/JNEUROSCI.1770-15.2016.
48. Fünfschilling U, Supplie LM, Mahad D, Boretius S, Saab AS, Edgar J, Brinkmann BG, Kassmann CM, Tzvetanova ID, Möbius W, Diaz F, Meijer D, Suter U, Hamprecht B, Sereda MW, Moraes CT, Frahm J, Goebbels S, Nave KA. Glycolytic oligodendrocytes maintain myelin and long-term axonal integrity. Nature. 2012 Apr 29;485(7399):517-21. doi: 10.1038/nature11007.
49. Gareau PJ, Rutt BK, Karlik SJ, Mitchell JR. Magnetization transfer and multicomponent T2 relaxation measurements with histopathologic correlation in an experimental model of MS. J Magn Reson Imaging. 2000 Jun;11(6):586-95. doi: 10.1002/1522-2586(200006)11:6<586::aid-jmri3>3.0.co;2-v.
50. Gudi V, Gingele S, Skripuletz T, Stangel M. Glial response during cuprizone-induced de- and remyelination in the CNS: lessons learned. Front Cell Neurosci. 2014 Mar 13;8:73. doi: 10.3389/fncel.2014.00073.
51. Gudi V, Moharregh-Khiabani D, Skripuletz T, Koutsoudaki PN, Kotsiari A, Skuljec J, Trebst C, Stangel M. Regional differences between grey and white matter in cuprizone induced demyelination. Brain Res. 2009 Aug 4;1283:127-38. doi: 10.1016/j.brainres.2009.06.005.
52. Guglielmetti C, Boucneau T, Cao P, Van der Linden A, Larson PEZ, Chaumeil MM. Longitudinal evaluation of demyelinated lesions in a multiple sclerosis model using ultrashort echo time magnetization transfer (UTE-MT) imaging. Neuroimage. 2020 Mar;208:116415. doi: 10.1016/j.neuroimage.2019.
53. Guglielmetti C, Veraart J, Roelant E, Mai Z, Daans J, Van Audekerke J, Naeyaert M, Vanhoutte G, Delgado Y Palacios R, Praet J, Fieremans E, Ponsaerts P, Sijbers J, Van der Linden A, Verhoye M. Diffusion kurtosis imaging probes cortical alterations and white matter pathology following cuprizone induced demyelination and spontaneous remyelination. Neuroimage. 2016 Jan 15;125:363-377. doi: 10.1016/j.neuroimage.2015.
54. Goodin DS. The epidemiology, pathology and pathogenesis of MS: Therapeutic implications. Neurotherapeutics. 2025 Jul;22(4):e00539. doi: 10.1016/j.neurot.2025.e00539.
55. Hertanu A, Soustelle L, Buron J, Le Priellec J, Cayre M, Le Troter A, Prevost VH, Ranjeva JP, Varma G, Alsop DC, Durbec P, Girard OM, Duhamel G. Inhomogeneous Magnetization Transfer (ihMT) imaging in the acute cuprizone mouse model of demyelination/remyelination. Neuroimage. 2023 Jan;265:119785. doi: 10.1016/j.neuroimage.2022.119785.

56. Hiehle JF Jr, Lenkinski RE, Grossman RI, Dousset V, Ramer KN, Schnall MD, Cohen JA, Gonzalez-Scarano F. Correlation of spectroscopy and magnetization transfer imaging in the evaluation of demyelinating lesions and normal appearing white matter in multiple sclerosis. Magn Reson Med. 1994 Sep;32(3):285-93. doi: 10.1002/mrm.1910320303.
57. Huynh JL, Garg P, Thin TH, Yoo S, Dutta R, Trapp BD, Haroutunian V, Zhu J, Donovan MJ, Sharp AJ, Casaccia P. Epigenome-wide differences in pathology-free regions of multiple sclerosis-affected brains. Nat Neurosci. 2014 Jan;17(1):121-30. doi: 10.1038/nn.3588.
58. Irvine KA, Blakemore WF. Remyelination protects axons from demyelination-associated axon degeneration. Brain. 2008 Jun;131(Pt 6):1464-77. doi: 10.1093/brain/awn080.
59. Jelescu IO, Zurek M, Winters KV, Veraart J, Rajaratnam A, Kim NS, Babb JS, Shepherd TM, Novikov DS, Kim SG, Fieremans E. In vivo quantification of demyelination and recovery using compartment-specific diffusion MRI metrics validated by electron microscopy. Neuroimage. 2016 May 15;132:104-114. doi: 10.1016/j.neuroimage.2016.02.004.
60. Jhelum P, Santos-Nogueira E, Teo W, Haumont A, Lenoël I, Stys PK, David S. Ferroptosis Mediates Cuprizone-Induced Loss of Oligodendrocytes and Demyelination. J Neurosci. 2020 Nov 25;40(48):9327-9341. doi: 10.1523/JNEUROSCI.1749-20.2020.
61. Kappos L, De Stefano N, Freedman MS, Cree BA, Radue EW, Sprenger T, Sormani MP, Smith T, Häring DA, Piani Meier D, Tomic D. Inclusion of brain volume loss in a revised measure of 'no evidence of disease activity' (NEDA-4) in relapsing-remitting multiple sclerosis. Mult Scler. 2016 Sep;22(10):1297-305. doi: 10.1177/1352458515616701.
62. Kates R, Atkinson D, Brant-Zawadzki M. Fluid-attenuated inversion recovery (FLAIR): clinical prospectus of current and future applications. Top Magn Reson Imaging. 1996 Dec;8(6):389-96. PMID: 9402679.
63. Keegan M, König F, McClelland R, Brück W, Morales Y, Bitsch A, Panitch H, Lassmann H, Weinshenker B, Rodriguez M, Parisi J, Lucchinetti CF. Relation between humoral pathological changes in multiple sclerosis and response to therapeutic plasma exchange. Lancet. 2005 Aug 13-19;366(9485):579-82. doi: 10.1016/S0140-6736(05)67102-4.
64. Kim JW, Choi J, Cho J, Lee C, Jeon D, Park SH. Preliminary Observations on Sensitivity and Specificity of Magnetization Transfer Asymmetry for Imaging Myelin of Rat Brain at High Field. Biomed Res Int. 2015;2015:565391. doi: 10.1155/2015/565391.

65. Kipp M, Nyamoya S, Hochstrasser T, Amor S. Multiple sclerosis animal models: a clinical and histopathological perspective. Brain Pathol. 2017 Mar;27(2):123-137. doi: 10.1111/bpa.12454.
66. Kipp M, van der Valk P, Amor S. Pathology of multiple sclerosis. CNS Neurol Disord Drug Targets. 2012 Aug;11(5):506-17. doi: 10.2174/187152712801661248.
67. Kitagawa S, Kufukihara K, Motegi H, Sekiguchi K, Sato Y, Nakahara J, q- Space Myelin Map: A new myelin-specific imaging technique for treatment monitoring of multiple sclerosis. Clinical and Exp Neuroimmun. 2024 Nov;15 (4). 169-176. doi: 10.1111/cen3.12796.
68. Klineova S, Lublin FD. Clinical Course of Multiple Sclerosis. Cold Spring Harb Perspect Med. 2018 Sep 4;8(9):a028928. doi: 10.1101/cshperspect.a028928.
69. Kornek B, Storch MK, Weissert R, Wallstroem E, Stefferl A, Olsson T, Linington C, Schmidbauer M, Lassmann H. Multiple sclerosis and chronic autoimmune encephalomyelitis: a comparative quantitative study of axonal injury in active, inactive, and remyelinated lesions. Am J Pathol. 2000 Jul;157(1):267-76. doi: 10.1016/S0002-9440(10)64537-3.
70. Krzyżak AT, Lasek J, Schneider Z, Wnuk M, Bryll A, Popiela T, Słowik A. Diffusion tensor imaging metrics as natural markers of multiple sclerosis-induced brain disorders with a low Expanded Disability Status Scale score. Neuroimage. 2024 Apr 15;290:120567. doi: 10.1016/j.neuroimage.2024.120567.
71. Krzyzak AT, Lasek J, Slowik A. Diagnostic performance of a multi-shell DTI protocol and its subsets with B-matrix spatial distribution correction in differentiating early multiple sclerosis patients from healthy controls. Front Neurol. 2025 Jul 28;16:1618582. doi: 10.3389/fneur.2025.1618582.
72. Ladopoulos T, Abbas Z, Krieger B, Bellenberg B, James JC, Bauer J, Gold R, Lukas C, Schneider R. Neurological disability and brain grey matter atrophy in primary progressive multiple sclerosis are determined by microstructural lesional changes, but not by lesion load. J Neurol. 2025 Apr 1;272(4):302. doi: 10.1007/s00415-025-13043-x.
73. Lassmann H, Bradl M. Multiple sclerosis: experimental models and reality. Acta Neuropathol. 2017 Feb;133(2):223-244. doi: 10.1007/s00401-016-1631-4.
74. Lassmann H, van Horssen J, Mahad D. Progressive multiple sclerosis: pathology and pathogenesis. Nat Rev Neurol. 2012 Nov 5;8(11):647-56. doi: 10.1038/nrneurol.2012.168
75. Laule C, Vavasour IM, Moore GR, Oger J, Li DK, Paty DW, MacKay AL. Water content and myelin water fraction in multiple sclerosis. A T2 relaxation study. J Neurol. 2004 Mar;251(3):284-93. doi: 10.1007/s00415-004-0306-6.
76. Laule C, Vavasour IM, Mädler B, Kolind SH, Sirrs SM, Brief EE, Traboulsee AL, Moore GR, Li DK, MacKay AL. MR evidence of long T2 water in pathological white matter. J Magn Reson Imaging. 2007 Oct;26(4):1117-21. doi: 10.1002/jmri.21132.

77. Laule C, Kozlowski P, Leung E, Li DK, Mackay AL, Moore GR. Myelin water imaging of multiple sclerosis at 7 T: correlations with histopathology. Neuroimage. 2008 May 1;40(4):1575-80. doi: 10.1016/j.neuroimage.2007.12.008.
78. Laule C, Moore GRW. Myelin water imaging to detect demyelination and remyelination and its validation in pathology. Brain Pathol. 2018 Sep;28(5):750-764. doi: 10.1111/bpa.12645.
79. Lee CH, Walczak P, Zhang J. Inhomogeneous magnetization transfer MRI of white matter structures in the hypomyelinated shiverer mouse brain. Magn Reson Med. 2022 Jul;88(1):332-340. doi: 10.1002/mrm.29207.
80. Li Y, Zhang Y, Han W, Hu F, Qian Y, Chen Q. TRO19622 promotes myelin repair in a rat model of demyelination. Int J Neurosci. 2013 Nov;123(11):810-22. doi: 10.3109/00207454.2013.804523.
81. Love S, Louis DN, Ellison DW. Greenfield's Neuropathology. 8th ed London: Hodder Arnold; 2008 ISBN 9780340906811.
82. Lubetzki C, Zalc B, Williams A, Stadelmann C, Stankoff B. Remyelination in multiple sclerosis: from basic science to clinical translation. Lancet Neurol. 2020 Aug;19(8):678-688. doi: 10.1016/S1474-4422(20)30140-X.
83. Lucchinetti C, Brück W, Parisi J, Scheithauer B, Rodriguez M, Lassmann H. Heterogeneity of multiple sclerosis lesions: implications for the pathogenesis of demyelination. Ann Neurol. 2000 Jun;47(6):707-17. doi: 10.1002/1531-8249(200006)47:6<707::aid-ana3>3.0.co;2-q.
84. Ludwin SK. Chronic demyelination inhibits remyelination in the central nervous system. An analysis of contributing factors. Lab Invest. 1980 Oct;43(4):382-7. PMID: 7442125.
85. MacKay A, Whittall K, Adler J, Li D, Paty D, Graeb D. In vivo visualization of myelin water in brain by magnetic resonance. Magn Reson Med. 1994 Jun;31(6):673-7. doi: 10.1002/mrm.1910310614.
86. MacKay AL, Laule C. Magnetic Resonance of Myelin Water: An in vivo Marker for Myelin. Brain Plast. 2016 Dec 21;2(1):71-91. doi: 10.3233/BPL-160033.
87. Maggi P, Macri SM, Gaitán MI, Leibovitch E, Wholer JE, Knight HL, Ellis M, Wu T, Silva AC, Massacesi L, Jacobson S, Westmoreland S, Reich DS. The formation of inflammatory demyelinated lesions in cerebral white matter. Ann Neurol. 2014 Oct;76(4):594-608. doi: 10.1002/ana.24242.
88. Manning AP, Chang KL, MacKay AL, Michal CA. The physical mechanism of "inhomogeneous" magnetization transfer MRI. J Magn Reson. 2017 Jan;274:125-136. doi: 10.1016/j.jmr.2016.11.013. Epub 2016 Nov 24. Erratum in: J Magn Reson. 2017 Sep;282:37. doi: 10.1016/j.jmr.2017.07.005.
89. McCreary CR, Bjarnason TA, Skihar V, Mitchell JR, Yong VW, Dunn JF. Multiexponential T2 and magnetization transfer MRI of demyelination and

remyelination in murine spinal cord. Neuroimage. 2009 May 1;45(4):1173-82. doi: 10.1016/j.neuroimage.2008.12.071.
90. McDonald WI, Compston A, Edan G, Goodkin D, Hartung HP, Lublin FD, McFarland HF, Paty DW, Polman CH, Reingold SC, Sandberg-Wollheim M, Sibley W, Thompson A, van den Noort S, Weinshenker BY, Wolinsky JS. Recommended diagnostic criteria for multiple sclerosis: guidelines from the International Panel on the diagnosis of multiple sclerosis. Ann Neurol. 2001 Jul;50(1):121-7. doi: 10.1002/ana.1032.
91. Mei F, Lehmann-Horn K, Shen YA, Rankin KA, Stebbins KJ, Lorrain DS, Pekarek K, A Sagan S, Xiao L, Teuscher C, von Büdingen HC, Wess J, Lawrence JJ, Green AJ, Fancy SP, Zamvil SS, Chan JR. Accelerated remyelination during inflammatory demyelination prevents axonal loss and improves functional recovery. Elife. 2016 Sep 27;5:e18246. doi: 10.7554/eLife.18246.
92. Merkler D, Boretius S, Stadelmann C, Ernsting T, Michaelis T, Frahm J, Brück W. Multicontrast MRI of remyelination in the central nervous system. NMR Biomed. 2005 Oct;18(6):395-403. doi: 10.1002/nbm.972.
93. Motegi H, Kufukihara K, Kitagawa S, Sekiguchi K, Hata J, Fujiwara H, Jinzaki M, Okano H, Nakamura M, Iguchi Y, Nakahara J. Non-lesional white matter changes depicted by q-space diffusional MRI correlate with clinical disabilities in multiple sclerosis. J Neurol Sci. 2024 Jan 15;456:122851. doi: 10.1016/j.jns.2023.122851.
94. Mottershead JP, Schmierer K, Clemence M, Thornton JS, Scaravilli F, Barker GJ, Tofts PS, Newcombe J, Cuzner ML, Ordidge RJ, McDonald WI, Miller DH. High field MRI correlates of myelin content and axonal density in multiple sclerosis--a post-mortem study of the spinal cord. J Neurol. 2003 Nov;250(11):1293-301. doi: 10.1007/s00415-003-0192-3.
95. Nakahara J. Visualization of Myelin for the Diagnosis and Treatment Monitoring of Multiple Sclerosis. Adv Exp Med Biol. 2019;1190:249-256. doi: 10.1007/978-981-32-9636-7_15.
96. Oakden W, Bock NA, Al-Ebraheem A, Farquharson MJ, Stanisz GJ. Early regional cuprizone-induced demyelination in a rat model revealed with MRI. NMR Biomed. 2017 Sep;30(9). doi: 10.1002/nbm.3743.
97. Omer N, Wilczynski E, Zlotzover S, Helft C, Blumenfeld-Katzir T, Ben-Eliezer N. Validation of a data-driven multicomponent T2 analysis for quantifying myelin content in the cuprizone mouse model of multiple sclerosis. PLoS One. 2025 May 21;20(5):e0323614. doi: 10.1371/journal.pone.0323614.
98. Van Obberghen E, Mchinda S, le Troter A, Prevost VH, Viout P, Guye M, Varma G, Alsop DC, Ranjeva JP, Pelletier J, Girard O, Duhamel G. Evaluation of the Sensitivity of Inhomogeneous Magnetization Transfer (ihMT) MRI for Multiple Sclerosis. AJNR Am J Neuroradiol. 2018 Apr;39(4):634-641. doi: 10.3174/ajnr.A5563.

99. Patrikios P, Stadelmann C, Kutzelnigg A, Rauschka H, Schmidbauer M, Laursen H, Sorensen PS, Brück W, Lucchinetti C, Lassmann H. Remyelination is extensive in a subset of multiple sclerosis patients. Brain. 2006 Dec;129(Pt 12):3165-72. doi: 10.1093/brain/awl217.
100. Peterson JW, Bö L, Mörk S, Chang A, Trapp BD. Transected neurites, apoptotic neurons, and reduced inflammation in cortical multiple sclerosis lesions. Ann Neurol. 2001 Sep;50(3):389-400. doi: 10.1002/ana.1123.
101. Plemel JR, Michaels NJ, Weishaupt N, Caprariello AV, Keough MB, Rogers JA, Yukseloglu A, Lim J, Patel VV, Rawji KS, Jensen SK, Teo W, Heyne B, Whitehead SN, Stys PK, Yong VW. Mechanisms of lysophosphatidylcholine-induced demyelination: A primary lipid disrupting myelinopathy. Glia. 2018 Feb;66(2):327-347. doi: 10.1002/glia.23245.
102. Pięd zia W, Jasiński K, Kalita K, Tomanek B, Węglarz WP. White and gray matter contrast enhancement in MR images of the mouse brain in vivo using IR UTE with a cryo-coil at 9.4 T. J Neurosci Methods. 2014 Jul 30;232:30-5. doi: 10.1016/j.jneumeth.2014.04.019.
103. Praet J, Guglielmetti C, Berneman Z, Van der Linden A, Ponsaerts P. Cellular and molecular neuropathology of the cuprizone mouse model: clinical relevance for multiple sclerosis. Neurosci Biobehav Rev. 2014 Nov;47:485-505. doi:10.1016/j.neubiorev.2014.10.004.
104. Preziosa P, Rocca MA, Mesaros S, Pagani E, Stosic-Opincal T, Kacar K, Absinta M, Caputo D, Drulovic J, Comi G, Filippi M. Intrinsic damage to the major white matter tracts in patients with different clinical phenotypes of multiple sclerosis: a voxelwise diffusion-tensor MR study. Radiology. 2011 Aug;260(2):541-50. doi: 10.1148/radiol.11110315.
105. Reich DS, Lucchinetti CF, Calabresi PA. Multiple Sclerosis. N Engl J Med. 2018 Jan 11;378(2):169-180. doi: 10.1056/NEJMra1401483.
106. Robson MD, Gatehouse PD, Bydder M, Bydder GM. Magnetic resonance: an introduction to ultrashort TE (UTE) imaging. J Comput Assist Tomogr. 2003 Nov-Dec;27(6):825-46. doi: 10.1097/00004728-200311000-00001.
107. Saab AS, Nave KA. Myelin dynamics: protecting and shaping neuronal functions. Curr Opin Neurobiol. 2017 Dec;47:104-112. doi: 10.1016/j.conb.2017.09.013.
108. Sachs HH, Bercury KK, Popescu DC, Narayanan SP, Macklin WB. A new model of cuprizone-mediated demyelination/remyelination. ASN Neuro. 2014 Sep 30;6(5):1759091414551955. doi: 10.1177/1759091414551955.
109. Schilling KG, Janve V, Gao Y, Stepniewska I, Landman BA, Anderson AW. Histological validation of diffusion MRI fiber orientation distributions and dispersion. Neuroimage. 2018 Jan 15;165:200-221. doi: 10.1016/j.neuroimage.2017.10.046.

110. Schirmer L, Möbius W, Zhao C, Cruz-Herranz A, Ben Haim L, Cordano C, Shiow LR, Kelley KW, Sadowski B, Timmons G, Pröbstel AK, Wright JN, Sin JH, Devereux M, Morrison DE, Chang SM, Sabeur K, Green AJ, Nave KA, Franklin RJ, Rowitch DH. Oligodendrocyte-encoded Kir4.1 function is required for axonal integrity. Elife. 2018 Sep 11;7:e36428. doi: 10.7554/eLife.36428.
111. Schmierer K, Wheeler-Kingshott CA, Boulby PA, Scaravilli F, Altmann DR, Barker GJ, Tofts PS, Miller DH. Diffusion tensor imaging of post mortem multiple sclerosis brain. Neuroimage. 2007 Apr 1;35(2):467-77. doi: 10.1016/j.neuroimage.2006.12.010.
112. Schneider T, Brownlee W, Zhang H, Ciccarelli O, Miller DH, Wheeler-Kingshott CG. Sensitivity of multi-shell NODDI to multiple sclerosis white matter changes: a pilot study. Funct Neurol. 2017 Apr/Jun;32(2):97-101. doi: 10.11138/fneur/2017.32.2.097.
113. Schoonheim MM, Geurts JJ, Barkhof F. The limits of functional reorganization in multiple sclerosis. Neurology. 2010 Apr 20;74(16):1246-7. doi: 10.1212/WNL.0b013e3181db9957
114. Schultz V, van der Meer F, Wrzos C, Scheidt U, Bahn E, Stadelmann C, Brück W, Junker A. Acutely damaged axons are remyelinated in multiple sclerosis and experimental models of demyelination. Glia. 2017 Aug;65(8):1350-1360. doi: 10.1002/glia.23167.
115. Serra-de-Oliveira N, Boilesen SN, Prado de França Carvalho C, LeSueur-Maluf L, Zollner Rde L, Spadari RC, Medalha CC, Monteiro de Castro G. Behavioural changes observed in demyelination model shares similarities with white matter abnormalities in humans. Behav Brain Res. 2015;287:265-75. doi: 10.1016/j.bbr.2015.03.038.
116. Serres S, Anthony DC, Jiang Y, Campbell SJ, Broom KA, Khrapitchev A, Sibson NR. Comparison of MRI signatures in pattern I and II multiple sclerosis models. NMR Biomed. 2009 Dec;22(10):1014-24. doi: 10.1002/nbm.1404.
117. Skripuletz T, Bussmann JH, Gudi V, Koutsoudaki PN, Pul R, Moharregh-Khiabani D, Lindner M, Stangel M. Cerebellar cortical demyelination in the murine cuprizone model. Brain Pathol. 2010 Mar;20(2):301-12. doi: 10.1111/j.1750-3639.2009.00271.x.
118. Skripuletz T, Gudi V, Hackstette D, Stangel M. De- and remyelination in the CNS white and grey matter induced by cuprizone: the old, the new, and the unexpected. Histol Histopathol. 2011 Dec;26(12):1585–97. doi: 10.14670/HH-26.1585.
119. Sled JG, Pike GB. Quantitative imaging of magnetization transfer exchange and relaxation properties in vivo using MRI. Magn Reson Med. 2001 Nov;46(5):923-31. doi: 10.1002/mrm.1278.
120. Sommer RC, Hata J, Rimkus CM, Klein da Costa B, Nakahara J, Sato DK. Mechanisms of myelin repair, MRI techniques and therapeutic opportunities in multiple sclerosis. Mult Scler Relat Disord. 2022 Feb;58:103407. doi: 10.1016/j.msard.2021.103407.

121. Sormani MP, Pardini M. Assessing Repair in Multiple Sclerosis: Outcomes for Phase II Clinical Trials. Neurotherapeutics. 2017 Oct;14(4):924-933. doi: 10.1007/s13311-017-0558-3.
122. Steinman L, Zamvil SS. Virtues and pitfalls of EAE for the development of therapies for multiple sclerosis. Trends Immunol. 2005 Nov;26(11):565-71. doi:10.1016/j.it.2005.08.014.
123. Tanikawa M, Nakahara J, Hata J, Suzuki S, Fujiyoshi K, Fujiwara H, Momoshima S, Jinzaki M, Nakamura M, Okano H, Takahashi S, Suzuki N. q-Space Myelin Map imaging for longitudinal analysis of demyelination and remyelination in multiple sclerosis patients treated with fingolimod: A preliminary study. J Neurol Sci. 2017 Feb 15;373:352-357. doi: 10.1016/j.jns.2017.01.009.
124. Thiessen, J.D., Zhang, Y., Zhang, H., Wang, L., Buist, R., Del Bigio, M.R., Kong, J., Li, X.-M. and Martin, M. (2013), Quantitative MRI and ultrastructural examination of the cuprizone mouse model of demyelination. NMR Biomed., 26: 1562-1581. https://doi.org/10.1002/nbm.2992.
125. Tomiak MM, Rosenblum JD, Prager JM, Metz CE. Magnetization transfer: a potential method to determine the age of multiple sclerosis lesions. AJNR Am J Neuroradiol. 1994 Sep;15(8):1569-74.
126. Trapp BD, Peterson J, Ransohoff RM, Rudick R, Mörk S, Bö L. Axonal transection in the lesions of multiple sclerosis. N Engl J Med. 1998 Jan 29;338(5):278-85. doi: 10.1056/NEJM199801293380502.
127. Tremlett H, Zhao Y, Joseph J, Devonshire V; UBCMS Clinic Neurologists. Relapses in multiple sclerosis are age- and time-dependent. J Neurol Neurosurg Psychiatry. 2008 Dec;79(12):1368-74. doi: 10.1136/jnnp.2008.145805.
128. Vargas WS, Monohan E, Pandya S, Raj A, Vartanian T, Nguyen TD, Hurtado Rúa SM, Gauthier SA. Measuring longitudinal myelin water fraction in new multiple sclerosis lesions. Neuroimage Clin. 2015 Sep 12;9:369-75. doi: 10.1016/j.nicl.2015.09.003.
129. Varma G, Girard OM, Prevost VH, Grant AK, Duhamel G, Alsop DC. In vivo measurement of a new source of contrast, the dipolar relaxation time, T1D , using a modified inhomogeneous magnetization transfer (ihMT) sequence. Magn Reson Med. 2017 Oct;78(4):1362-1372. doi: 10.1002/mrm.26523.
130. Vavasour IM, Whittall KP, MacKay AL, Li DK, Vorobeychik G, Paty DW. A comparison between magnetization transfer ratios and myelin water percentages in normals and multiple sclerosis patients. Magn Reson Med. 1998 Nov;40(5):763-8. doi: 10.1002/mrm.1910400518.
131. Vavasour IM, Laule C, Li DK, Traboulsee AL, MacKay AL. Is the magnetization transfer ratio a marker for myelin in multiple sclerosis? J Magn Reson Imaging. 2011 Mar;33(3):713-8. doi: 10.1002/jmri.22441.

132. Vrenken H, Geurts JJ, Knol DL, Polman CH, Castelijns JA, Pouwels PJ, Barkhof F. Normal-appearing white matter changes vary with distance to lesions in multiple sclerosis. AJNR Am J Neuroradiol. 2006 Oct;27(9):2005-11. PMID: 17032884.
133. van Waesberghe JH, Kamphorst W, De Groot CJ, van Walderveen MA, Castelijns JA, Ravid R, Lycklama à Nijeholt GJ, van der Valk P, Polman CH, Thompson AJ, Barkhof F. Axonal loss in multiple sclerosis lesions: magnetic resonance imaging insights into substrates of disability. Ann Neurol. 1999 Nov;46(5):747-54. doi: 10.1002/1531-8249(199911)46:5<747::aid-ana10>3.3.co;2-w.
134. Walton C, King R, Rechtman L, Kaye W, Leray E, Marrie RA, Robertson N, La Rocca N, Uitdehaag B, van der Mei I, Wallin M, Helme A, Angood Napier C, Rijke N, Baneke P. Rising prevalence of multiple sclerosis worldwide: Insights from the Atlas of MS, third edition. Mult Scler. 2020 Dec;26(14):1816-1821. doi: 10.1177/1352458520970841.
135. Wang X, Cusick MF, Wang Y, Sun P, Libbey JE, Trinkaus K, Fujinami RS, Song SK. Diffusion basis spectrum imaging detects and distinguishes coexisting subclinical inflammation, demyelination and axonal injury in experimental autoimmune encephalomyelitis mice. NMR Biomed. 2014 Jul;27(7):843-52. doi: 10.1002/nbm.3129.
136. Wergeland S, Torkildsen Ø, Myhr KM, Mørk SJ, Bø L. The cuprizone model: regional heterogeneity of pathology. APMIS. 2012 Aug;120(8):648-57. doi: 10.1111/j.1600-0463.2012.02882.x.
137. Wiggermann V, Endmayr V, Hernández-Torres E, Höftberger R, Kasprian G, Hametner S, Rauscher A. Quantitative magnetic resonance imaging reflects different levels of histologically determined myelin densities in multiple sclerosis, including remyelination in inactive multiple sclerosis lesions. Brain Pathol. 2023 Nov;33(6):e13150. doi: 10.1111/bpa.13150.
138. Wu GF, Alvarez E. The immunopathophysiology of multiple sclerosis. Neurol Clin. 2011 May;29(2):257-78. doi: 10.1016/j.ncl.2010.12.009.
139. Wuerfel J, Tysiak E, Prozorovski T, Smyth M, Mueller S, Schnorr J, Taupitz M, Zipp F. Mouse model mimics multiple sclerosis in the clinico-radiological paradox. Eur J Neurosci. 2007 Jul;26(1):190-8. doi: 10.1111/j.1460-9568.2007.05644.x.
140. Young IR, Hall AS, Pallis CA, Legg NJ, Bydder GM, Steiner RE. Nuclear magnetic resonance imaging of the brain in multiple sclerosis. Lancet. 1981 Nov 14;2(8255):1063-6. doi: 10.1016/s0140-6736(81)91273-3.
141. Zhan J, Mann T, Joost S, Behrangi N, Frank M, Kipp M. The Cuprizone Model: Dos and Do Nots. Cells. 2020 Mar 31;9(4):843. doi: 10.3390/cells9040843.
142. Zhang L, Wen B, Chen T, Tian H, Xue H, Ren H, Li L, Fan Q, Ren Z. A comparison study of inhomogeneous magnetization transfer (ihMT) and magnetization transfer (MT) in multiple sclerosis based on whole brain acquisition at 3.0 T. Magn Reson Imaging. 2020 Jul;70:43-49. doi: 10.1016/j.mri.2020.03.010.

143. Zhen W, Liu A, Lu J, Zhang W, Tattersall D, Wang J. An Alternative Cuprizone-Induced Demyelination and Remyelination Mouse Model. ASN Neuro. 2017 Jul-Aug;9(4):1759091417725174. doi: 10.1177/1759091417725174.
144. Zirngibl M, Assinck P, Sizov A, Caprariello AV, Plemel JR. Oligodendrocyte death and myelin loss in the cuprizone model: an updated overview of the intrinsic and extrinsic causes of cuprizone demyelination. Mol Neurodegener. 2022 May 7;17(1):34. doi: 10.1186/s13024-022-00538-8.
145. Zivadinov R, Stosic M, Cox JL, Ramasamy DP, Dwyer MG. The place of conventional MRI and newly emerging MRI techniques in monitoring different aspects of treatment outcome. J Neurol. 2008 Mar;255 Suppl 1:61-74. doi: 10.1007/s00415-008-1009-1.